Bulletin of Earthquake Engineering, 11(6), 2013, 2007-2032

Capacity, fragility and damage in reinforced concrete buildings: a probabilistic approach.

Yeudy F. Vargas,[a] Luis G. Pujades, [a] [b] Alex H. Barbat,[a] and Jorge E. Hurtado[c]

Abstract

The main goals of this article are the analysis of the use of simplified deterministic nonlinear static procedures to assess the seismic response of buildings, and to evaluate the influence that the uncertainties regarding the mechanical properties of the materials and of the features of the seismic actions have in the uncertainties of the structural response. A current reinforced concrete building is used as a guiding case study. In the calculation of the expected spectral displacement, deterministic static methods are simple and straightforward. In the case of non severe earthquakes, these approaches lead to somewhat conservative but adequate results when compared to more sophisticated procedures involving non-linear dynamic analyses. Concerning the probabilistic assessment, the strength properties of the materials, concrete and steel, and the seismic action are considered as random variables. The Monte Carlo method is then used to analyze the structural response of the building. The obtained results show that significant uncertainties are expected, as uncertainties in the structural response increase with the severity of the seismic actions. The major influence in the randomness of the structural response comes from the randomness of the seismic action. A useful example for selected earthquake scenarios is used to show the applicability of the probabilistic approach to assess the expected damage and risk analysis. An important conclusion of this work is the need to address the fragility of the buildings and expected damage assessment problem from a probabilistic perspective.

[a] Universitat Politècnica de Catalunya-BarcelonaTech (UPC).

[b] Corresponding autor. e-mail: lluis.pujades@upc.edu.

[c] Universidad Nacional de Colombia en Manizales.

Bulletin of Earthquake Engineering, 11(6), 2013, 2007-2032

1 Introduction

More than two thousand years ago, Vitruvius (1 BC) already stated that architecture is the merging of functionality, strength and beauty. Since the last decade of the twentieth century, the performance based design has been an important engineering outcome, becoming a sign of the advances in building construction that mainly concerns functionality and strength. Therefore, strength and functional requirements are integrated into building design, being the performance of the building the result of the interaction among different subsystems, including the structural system (SEAOC Vision 2000 Committee, 1995). Modern building regulations and design codes are based on performance principles and they incorporate, among many others, requirements for structural safety, including earthquake resistance. In the case of earthquakes, the capacity spectrum method (Freeman *et al.* 1975, Freeman 1978, 1998) allows characterizing the interaction between the seismic demand, and the building. Simplified procedures allow determining the displacement demand imposed on a building expected to deform inelastically (ATC, 1996, FEMA, 1997). Additionally, in order to analyze the seismic risk of existing buildings, several simplified methods were developed. ATC-13 (ATC, 1985) and ATC-25 (ATC, 1996) define the earthquake by means of macroseismic MM intensities and develop damage probability matrices for 75 facility classes. ATC-13 and ATC-25 methods are based on expert opinion. Moreover, vulnerability index-based methods define the seismic action also by means of macroseismic intensities (EMS-98, Grünthal 1998), but the structure is defined through a vulnerability index (Barbat *et al.* 1996; Barbat *et al.* 1998). More recently, capacity spectrum-based methods were also adopted to assess the seismic risk of existing buildings (FEMA, 1999, McGuire, 2004). Capacity Spectrum-Based Methods (CSBM) define the building by means of a Pushover Analysis (PA) curve, called capacity curve, which represents base shear forces as a function of roof displacements while the earthquake is defined by the corresponding 5% damped elastic response spectrum. In those cases in which the response of the structure is dominated by the fundamental mode of vibration, base shear forces and roof displacements are converted into the spectral accelerations and spectral displacements of an equivalent Single Degree of Freedom (SDOF) system respectively. These spectral values define the so-called capacity spectra (Fajfar, 1999) also called capacity diagrams (Chopra and Goel 1999). The earthquake ground motions requirements are then defined by highly damped elastic response spectra. In the Acceleration Displacement Response Spectrum (ADRS) format, spectral accelerations are plotted as a function of the spectral dis-

placement with the periods represented by radial lines. The intersection of the capacity spectrum and the demand spectrum provides an estimate of the inelastic acceleration and displacement requirement (Fajfar 1999). In CSBM vulnerability is defined by fragility curves that define the probability that a determined damage state be equaled or exceeded as a function of a parameter related to the intensity of the seismic demand. Generally the Spectral displacement (*Sd*) is used to define the size of the seismic demand. Four non-null damage grades or Damage states (ds_i) are usually considered (FEMA 1999): ds_1) Slight, ds_2) Moderate, ds_3) Extensive and ds_4) Complete. Each Fragility Curve (FC_i) is defined by means of a cumulative lognormal distribution function, which is fully defined by two parameters, namely the median value, μ, and the standard deviation, β. For large-scale assessments of seismic damage and risk, simplified procedures were proposed to define these two parameters. Median values are derived from the capacity spectrum in its bilinear simplified form, while standard deviations are obtained assuming that the damage in earthquakes is distributed according to a binomial probability distribution (Lagomarsino & Giovinazzi, 2006). These simplified procedures were applied to different building types and cities. See for instance Barbat *et al.* (2008); Lantada *et al.* (2009) and Pujades *et al.* (2011). However, all these risk studies are deterministic, in the sense that they do not take into account the uncertainties, neither epistemic nor random, of the parameters involved. Non-Linear Dynamic Analysis (NLDA) consists in submitting the structure to acceleration time-histories, which can be defined by synthetic or recorded accelerograms. This more sophisticated and costly structural analysis allows observing the time-histories of the structural response, being frequently used for comparison between the maximum values obtained and the ones coming from more straightforward static methods (see Mwafy & Elnashai 2000; Poursha *et al.* 2007 and Kim & Kuruma 2008). It is worth noting that in these works the problem is not either faced from a probabilistic viewpoint. Among many others authors, McGuire (2004) emphasizes the importance of dealing with seismic risk assessment from a probabilistic point of view. Actually there are many sources of randomness due to random and epistemic uncertainties. A number of issues concerning the impact of epistemic uncertainties on earthquake loss models is described and discussed in some detail in Crowley *et al.* (2005). Most of the parameters involved in the assessment of seismic vulnerability and risk of structures are random variables. Concerning the structure itself, a few examples are the parameters related to the characteristics of the materials, geometry and size of the structure and of the sections of its structural elements, cracking and crushing of concrete,

strain hardening and ultimate strength of steel, as well as many other effects such as slab participation and axial force variations on column strength. Moreover, an additional significant source of randomness is the expected seismic action. Therefore, effective peak acceleration, peak ground acceleration (PGA), frequency content and duration are random variables that introduce significant uncertainties in the structural response. To overcome this high variability in a deterministic simplified way, seismic design standards suggest using decreased material strengths and increased seismic actions. Convenient safety factors are recommended. However, it is well known that in a non-linear system it is not guaranteed that a variation in the input parameters would produce a similar variation in the output parameters response. Consequently the probability distribution of the response might be different from that corresponding to the input variables. Therefore, increasing the severity of the expected seismic actions and decreasing strength parameters do not ensure the reliability of the response. Moreover, these conservative assumptions may lead to excessively conservative responses. Accordingly, it could be concluded that it is correct to face structural analysis and seismic risk analysis by using probabilistic approaches. Borzi *et al.* (2007) treat the strength parameters and dimensions of structural capacity as being random. Fragiadakis & Vamvatsikos (2010) evaluate the nonlinear behavior of structures by means of nonlinear static analysis. They took into account the uncertainties of the properties of the materials, by using a Monte Carlo procedure. Dolsek (2010) considered the randomness of the seismic action using real earthquake accelerograms compatible with target design spectra, but did not take into account the uncertainties of the mechanical properties of the structure. The main goals of this article are the following: (1) the analysis of the use of simplified nonlinear static procedures to assess the seismic response of buildings when compared to more sophisticated and costly NLDA methods; (2) to analyze the influence of the uncertainties in the structural response produced by the uncertainties in the structural properties and in the seismic actions. Concerning structural properties, for the sake of simplicity, only the randomness of steel yield strength and the concrete compressive strength are considered by means of adequate probability distributions. The uncertainties in the seismic actions are considered by means of sets of accelerograms corresponding to real earthquakes whose response spectra fit well the design spectra chosen for the analysis. A reinforced concrete building with waffle slabs is used as a guiding case study. This type of building is frequently used in Spain as multifamily housing, being well known its limited ductility (Vielma *et al.* 2009; Vielma *et al.* 2010). A simplified capacity spectrum-based method is

then used to assess the fragility and expected damage of this building. The seismic response of this building is also investigated by means of NLDA. Both analyses, static and dynamic, are carried out by means of deterministic and probabilistic approaches. The Ruaumoko software (Carr 2000) is used for the computations involved in the structural analyses. The results are then used for comparison and discussion.

2 Building and building model

The building used as a guiding case-study is a reinforced concrete building with waffle slabs. As stated above, these buildings have limited ductility and are very frequent in Spain and other Mediterranean countries. The building has 8 stories and 6 spans (see Figure 1), and it is composed of pillars and waffle slabs. Additionally, some details of the construction of waffle slabs can be seen in Figure 1. However, in the numerical model of the building, waffle slabs are approximated by beams with equivalent inertia. Moreover, it is assumed that structural elements, beams and pillars, follow the Takeda (Otani 1974) hysteretic rule. Yield surfaces are defined by the interaction diagram of the bending moment and the axial load of the pillars, and the bending moment curvature in beams. Loads are applied following the recommendations of Eurocode 8 (EC08 2004) for reinforced concrete structures. The Rayleigh or proportional damping model is used.

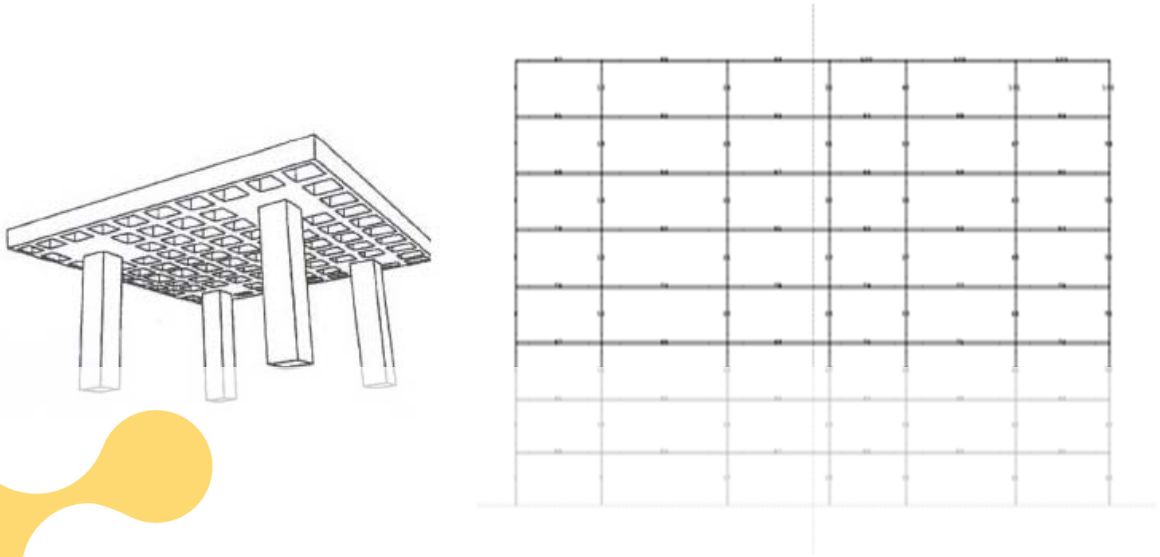

Figure 1. Examples of waffle slab construction details (up left, source: the authors), waffle slab sketch (down left; source: Villalba, 2006) and building model. The main dimensions of the building are: H = 25.65 m, B = 24 m and the fundamental period is T = 1.44 s.

Strength properties of construction materials are usually obtained in the quality control during their manufacture and/or during the construction works. In the case of steel yield strength and concrete compressive strength these values are obtained from tension and compression tests in samples of steel and concrete, respectively. By means of these tests, the strength of materials can be described as a random variable. On this basis, the concrete compressive strength (*fc*) and the steel yield strength (*fy*) are modeled as normal random variables. Table 1 shows the corresponding mean, μ, standard deviation, σ, and coefficient of variation (c.o.v.). The coefficient of variation (c.o.v.) of a random variable is the ratio between its standard deviation and its mean value. For deterministic approaches, design standards suggest using characteristic values for the strength of the materials. The characteristic value is defined as the one having an exceedance probability equal to 0.95. For normal probability distributions, the following equations define the characteristic values, $f'c$ and $f'y$, of fc and fy respectively.

$$f'c = \mu_{f_c} - 1.65\,\sigma_{f_c}$$
$$f'y = \mu_{f_y} - 1.65\,\sigma_{f_y} \qquad (1)$$

Table 1. Mean values (μ), standard deviations (σ) and coefficients of variation of the concrete compressive strength (*fc*) and the steel yield strength (*fy*) considered as normal random variables.

	μ (MPa)	σ (MPa)	Coefficient of variation (c.o.v.)
fc	30	1.5	0.05
fy	420	21	0.05

Thus, values in Table 1 and Equations (1) allow obtaining characteristic strength values of materials for concrete ($f'c$=27525 kPa) and steel ($f'y$=385350 kPa). These characteristic values were used in the deterministic approach, while the normal probability distributions defined by the parameters in Table 1 were used in the probabilistic approach by using Monte Carlo simulations.

3 Seismic action

It is worth noting that for application to specific urban areas, the earthquake scenarios and the corresponding seismic actions should be defined according to the seismic hazard of the zone. This means that, according to the regional and local seismic hazard available studies, adequate response spectra and likely expected PGA values must be used. Anyhow, this is not the purpose of this study, in which the 5% damped elastic response spectra provided in Eurocode EC08 are tested and a wide range of PGA are used in such a way that the structural response can be analyzed for spectral displacements in the range between the elastic behavior and the collapse. Nonlinear static procedures require defining the seismic actions by means of 5% damped elastic response spectra. NLDA require acceleration time histories, namely accelerograms. The comparison of the results obtained requires for the acceleration time histories used in dynamic analyses to be compatible with the response spectra used in static procedures. There are several ways to tackle this issue. One solution is to use synthetic accelerograms compatible with the response spectrum. In fact, Ruaumoko software incorporates tools (Gasparini and Vanmarcke 1976) to produce synthetic accelerograms compatible with a given response spectrum. Another option is to use real accelerograms. Hancock *et al.* (2008) provide an overview of the different approaches to use real accelerograms. The choice is not straightforward as there are many legitimate options between these two alternatives, including scaling real accelerograms to adequate periods or range of periods, or using spectral

matching techniques. Anyhow, for seismic damage and risk assessment, Faccioli (2006) and Faccioli and Pessina (2003) recommend the use of accelerograms of actual earthquakes and this choice was preferred in this work. A specific method for the selection of a number of accelerograms, from accelerogram databases compatible with a given response spectrum, is proposed in this paper and will be described below. But before that, the response spectra used in this paper are described.

3.1 Response spectra

Eurocode EC08 provides two kinds of elastic response spectra, type 1 and type 2, respectively for great (M_s>5.5) and small earthquakes, and five soil classes: A, B, C, D, and E. Class A corresponds to the hardest soils and class D to the softest ones. Class E corresponds to special soils with stratified heterogeneous sediments. These spectra will be referred as 1A, 1B, 1C, 1D and 1E, and 2A, 2B, 2C, 2D and 2E. The normalized spectral shapes of these spectra are shown in Figure 1. Extreme spectra 1A, 1D, 2A and 2D have been highlighted and the values corresponding to the fundamental period of the building (T = 1.44 s) were also plotted in this figure. These four extreme spectra will be used in non linear static analyses. It can be seen how, at this period, the 1D spectrum has the highest response, so in NLDA it is expected that the accelerograms most damaging the structure will be those matching this spectrum. Furthermore, the spectral ordinate of the 2D spectrum is a little bit higher than that corresponding to the 1A spectrum. Note how the static and dynamic structural analyses will confirm that the spectral displacements and expected damage are greater for the seismic actions defined by 1D and 2D spectra than for the ones defined by 1A and 2A spectra respectively.

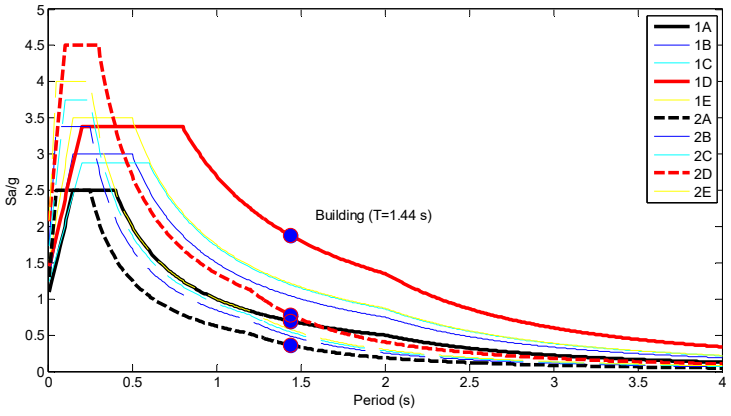

Figure 2. Normalized spectral shapes of the 5% damped elastic response spectra provided in Euro-

code EC08. Circle markers indicate the spectral responses for 1A, 1D, 2A and 2D spectra corresponding to the fundamental period (T = 1.44 s) of the building.

Moreover, as we will see later on, supplementary work has shown that for low PGA values, the seismic inputs that produce the greatest spectral displacements are those matching the 1D spectrum. The spectral displacement of the ultimate point of the capacity spectrum of the building considered is 21.2 cm. To get this spectral displacement, using seismic actions defined by the rest of spectra, it would be necessary to scale acceleration records to large PGA values, greater than 0.6 g, which are highly unlikely in Spain, where the PGA for a return period of 500 years is less than 0.25 g (NCSE-02, 2002). Therefore, in this paper the Incremental Dynamic Analysis (IDA), both probabilistic and deterministic, will be performed only using records whose response spectra are compatible with the 1D spectrum. This analysis was considered sufficient for the purpose of this work. In the following section a specific procedure is proposed to select accelerograms. That is, given a target spectrum and an accelerograms database, the purpose is to extract the optimum number of accelerograms of the database better fitting the target spectrum.

3.2 Accelerograms

As stated before, NLDA requires accelerograms. Stochastic analyses require a significant number of accelerograms, all of them well-matched with the target spectrum. Given a target response spectrum and a specific database of acceleration records, the procedure used to select accelerograms observes the following steps. Step 1: normalize the target spectrum at period zero. Step 2: compute the corresponding normalized spectrum for each accelerogram. Step 3: compute a measure of the misfit between the computed and target spectra; in this case, this measure is the error computed according to the following equation:

$$\varepsilon_j = \frac{1}{n-1}\sqrt{\sum_{i=1}^{n_j}\left(y_{ji} - Y_i\right)^2} \quad j = 1 \cdots N, \qquad i = 1 \cdots n \tag{2}$$

where ε_j is a least square measure of the misfit between the spectrum of accelerogram j and the target spectrum, $y_{i,j}$ is spectral ordinate i of the spectrum of accelerogram j, and Y_i is the corresponding i ordinate of the target spectrum; n is the number of spectral ordinates of the accelerogram, which are assumed to be the same for each accelerogram j, and N is the number of accelerograms. Step 4: organize spectra according to increasing errors. Step 5: let

Sa_{ik} $i=1\cdots n, k=1\cdots N$, be the i spectral ordinates corresponding to the spectrum of accelerogram k, once the accelerogram series have been arranged in such a way that $\varepsilon_k \le \varepsilon_{(k+1)}$ $k=1\cdots N-1$. Step 5: compute the following new spectra:

$$b_{im} = \frac{1}{m}\sum_{k=1}^{m} Sa_{ik} \qquad i=1\cdots n, \quad m=1\cdots N; \tag{3}$$

b_{im} is now the spectral ordinate of the mean of the first m spectra, once they have been arranged. Step 6: compute the following new error function (Er_m) which is similar to that given in Equation (2).

$$Er_m = \frac{1}{n-1}\sqrt{\sum_{i=1}^{n_m}\left(b_{im}-Y_i\right)^2} \quad m=1\cdots N, \qquad i=1\cdots n \tag{4}$$

The value of m that minimizes the value of Er_m is taken as the optimum number of accelerograms that are compatible with the given target spectrum and that can be used from the given database. Of course the value of Er_1 is also crucial to know the adequacy of the fit. For databases with a large number of accelerograms, Er_1 is really low, while there are m values of the order of several tens. Some additional basic assumptions can be made in order to reduce the size of the database. Information about the magnitude and focal mechanism of earthquakes and about distance and soil type of accelerometric stations can be used to significantly reduce the number of acceleration records to be tested. This procedure was applied to the European (Ambraseys *et al.* 2002, Ambraseys *et al.* 2004) and Spanish strong motion databases. As the European database is larger, most of the selected accelerograms are taken from this database. Nevertheless, for spectra type 2, some additional accelerograms were selected from the Spanish database. For each spectrum, 1A, 1D, 2A and 2D, more than 1000 acceleration records were tested. Figure 3 shows the error function, Er_m in Equation (4), for EC08 1D spectrum. The value of m minimizing this function was found to be 20. Table 2 shows the main parameters of these accelerograms. The mean values of magnitude, distance and depth are respectively 6.5, 67 km and 16.7 km, and the corresponding standard deviations are 0.7, 53.6 km and 17.6 km. Figure 4 a) shows the target EC08 1D spectrum, the mean spectrum and the spectrum defined by the median values plus one standard deviation. The fundamental period of the building is also plotted in this figure. Figure 4 b) shows an example of compatible accelerogram. Table 3 shows the statistics of the distributions of the magnitudes of the events

corresponding to the accelerograms that were selected for their compatibility with 1A, 1D, 2A and 2D spectra.

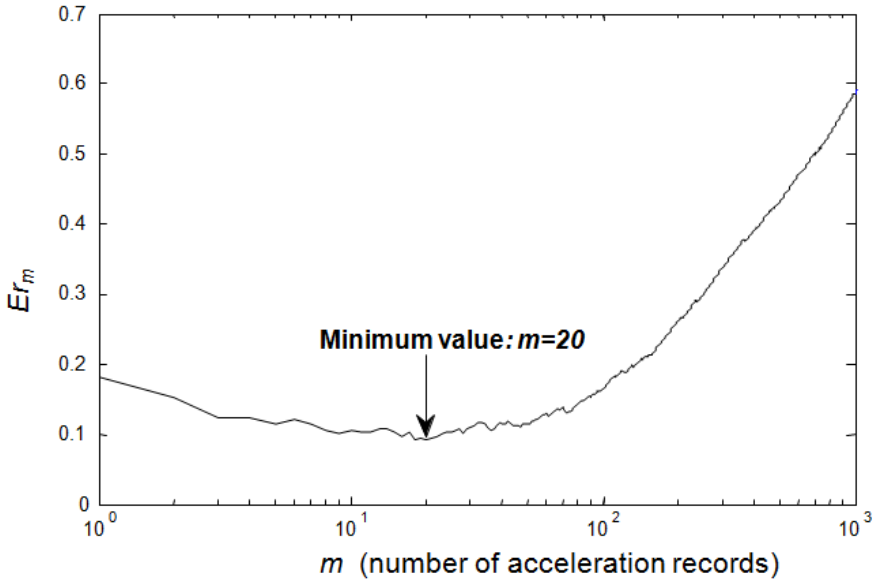

Figure 3. Function Er_m used to optimize the number of compatible accelerograms. This example corresponds to EC08, 1D spectrum and m = 20. The main parameters of the selected records are shown in Table 2.

4 Deterministic approach

The capacity, fragility and expected damage of the building whose structural model has been described in the previous section are first estimated by means of a deterministic approach.

4.1 Nonlinear static analysis

In this case the characteristic values given above are used; see Equation (1) and Table 1. Nonlinear static analysis or Pushover Analysis (PA) consists in simulating the horizontal loads according to a specific pattern and then increasing their values until the structure collapses. The result of PA is the capacity curve shown in Figure 5 a), which represents the shear force at the base as a function of the displacement at the roof of the building (see also Mata *et al.* 2007; Faleiro *et al.* 2008). The loading pattern (triangular, rectangular, and so on) has a major influence on the results (Mwafy & Elnashai 2000).

Table 2. Main parameters of the 1D spectrum compatible accelerograms.

Event n.	*Date*	*Epicenter (deg)*		*Depth (km)*	*Mag.*	*M. type*	*Station name*	*Distance (km)*
		Lat N	*Lon E*					

1	06.05.1976	46.32	13.32	6	6.3	Mw	Castelfranco-Veneto	132
2	06.05.1976	46.32	13.32	6	6.3	Mw	Codroipo	48
3	15.09.1976	43.32	13.16	12	5.9	Mw	Cortina d´Ampezzo	83
4	16.09.1978	33.36	57.42	5	7.3	Ms	Boshroyeh	55
5	15.04.1979	41.98	18.98	12	7.0	Ms	Ulcinj-Hotel Olimpic	24
6	23.11.1980	47.78	15.33	16	6.5	Mw	Bagnoli-Irpino	23
7	23.11.1980	47.78	15.33	16	6.5	Mw	Rionero in Vulture	33
8	23.11.1980	47.78	15.33	16	6.5	Mw	San Giorgio la Molara	64
9	17.01.1983	38.07	20.25	14	7.0	Ms	Agrinio-Town Hall	118
10	06.06.1986	38.01	37.91	11	5.7	Ms	Galbasi-Devlet Hastanesi	34
11	13.09.1986	37.10	22.18	8	5.7	Ms	Kalamalata-Prefecture	9
12	30.05.1990	45.85	26.66	89	6.8	Ms	Istrita	80
13	20.06.1990	39.96	49.41	19	7.3	Ms	Tehran-Sarif University	223
14	20.06.1990	39.96	49.41	19	7.3	Ms	Tonekabun	131
15	06.11.1992	38.16	27.00	17	6.0	Ms	Izmir-Bayindirlik	30
16	26.09.1997	43.02	12.89	7	5.7	Mw	Bevagna	25
17	09.11.1997	42.90	12.95	10	4.8	Mb	Castelmuovo-Assisi	31
18	23.11.1980	40.78	15.33	16	6.5	Mw	Gioia-Sannitica	94
19	17.08.1999	40.70	29.99	17	7.4	Mw	Bursa-Sivil Savunma	93
20	17.08.1999	40.70	29.99	17	7.4	Mw	Izmit-Metereoloji-Istasyonu	10

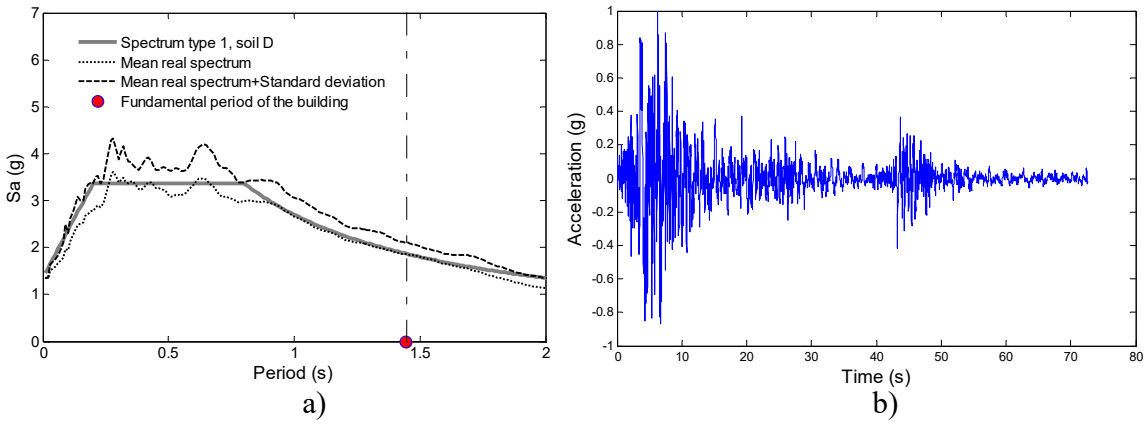

a) b)

Figure 4. a) Normalized EC08 1D spectrum. The mean and the mean plus one standard deviation spectra are also shown. The fundamental period of the structure is also plotted. b) Example of one accelerogram matching this spectrum.

The Adaptive Pushover Analysis (APA) technique proposed by Satyarno (1999) has been used in this work. A detailed description of this procedure can be found in the Ruaumoko software manuals (Carr 2000). Figure 5 a) shows the capacity curve and Figure 5 b) shows the capacity spectrum and its bilinear simplified form (ATC-40 1996), which is defined by the yielding point (Dy, Ay) and the ultimate capacity point (Du, Au). In this case, Dy = 0.13 m, Ay = 0.23 g, Du = 0.21 m and Au = 0.24 g. Dy and Du, are used to elaborate fragility curves by means of a simplified procedure.

Table 3. Statistics: mean values, standard deviations and coefficients of variation of the magnitudes of the earthquakes corresponding to the selected accelerograms and spectra.

EC08 spectrum type	Mean value (μ_M)	Standard deviation (σ_M)	Coef. of var. c.o.v.
1A	5.5	1.22	0.20
1D	6.5	0.72	0.11
2A	5.3	0.82	0.16
2D	5.2	0.99	0.19

4.2 Fragility curves

As stated above, for a building or a structure and for a given damage state ds_i, the corresponding fragility curve defines the probability that this damage state be equaled or exceeded. This function is defined by a cumulative lognormal distribution, as a function of a parameter defining the intensity of the seismic action (FEMA 1999), which in our case is the spectral displacement (Sd).

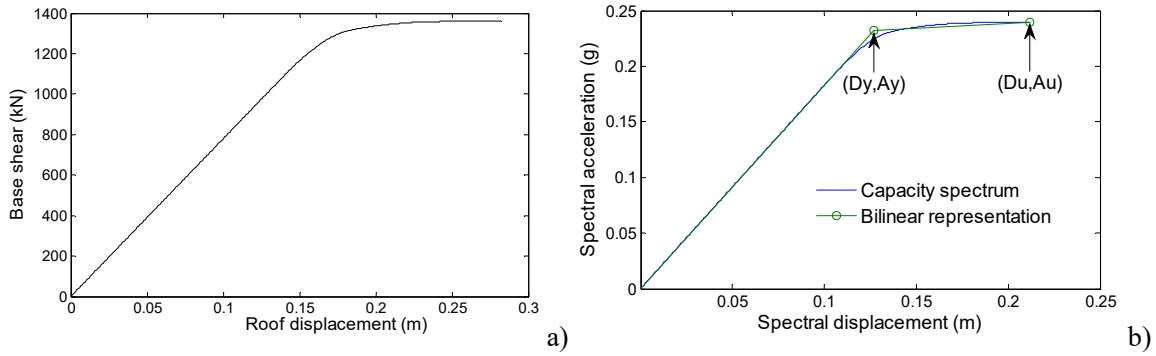

a) b)

Figure 5. Capacity curve (a) and capacity spectrum (b) obtained from the deterministic APA.

The normal and lognormal distributions are closely related. If X is distributed lognormally with parameters μ and σ, then log(X) is distributed normally with mean μ and standard deviation σ. In our case, the following equation defines the fragility curve (FEMA 1999):

$$P\left[d \geq ds_i \left| Sd \right.\right] = \varphi\left[\frac{1}{\beta_{ds_i}} Ln\left(\frac{Sd}{\overline{Sd}_{ds_i}}\right)\right] \tag{5}$$

where φ stands for the cumulative lognormal distribution, d is the expected damage, Sd is the spectral displacement, and $\overline{Sd}_{ds_i}$ and β_{ds_i} are the median values and standard deviations of the corresponding normal distributions. For simplicity $\overline{Sd}_{ds_i}$ will be called as μ_{ds_i}. μ_{ds_i} is also known as the damage state threshold, and the probability of exceedance of the damage state

ds_i for $Sd = \mu_{ds_i}$ is equal to 0.5. The following simplified assumptions allow obtaining fragility curves from the bilinear form of the capacity spectrum: 1) μ_{ds_i} is related to the yielding point and ultimate capacity point as follows:

$$\mu_{ds_1} = 0.7Dy, \quad \mu_{ds_2} = Dy, \quad \mu_{ds_3} = Dy + 0.25\,(Du - Dy), \quad \text{and } \mu_{ds_4} = Du \tag{6}$$

and 2) the expected seismic damage in buildings follows a binomial probability distribution. These assumptions were proposed by Lagomarsino and Giovinazzi in the framework of the Risk-UE project (Milutinovic & Trendafiloski, 2003), were published by Lagomarsino and Givinazzi (2006) and have been used in many seismic risk assessment studies for European earthquake prone cities (see for instance Barbat *et al.* 2008 and Pujades *et al.* 2012). The first assumption is based on expert opinion and relates the expected damage to the stiffness degradation of the structure; the second one is based on the damage observed in past earthquakes. In fact, the European Macroseismic Scale, EMS'98 (Grünthal 1998), establishes that the observed damage follows a binomial distribution. Given that for the damage states thresholds, the probability of exceedance of the corresponding damage state is 50%, assuming the binomial distribution allows calculating the probabilities of exceedance of the other damage states. Therefore β_{ds_i} can be obtained from a least squares fit of the fragility curves to the computed exceedance probabilities, thus defining the fragility curves completely. A more detailed description on how the values of β_{ds_i} are obtained can be found in Lantada *et al.* (2009). Figure 6 shows the deterministic fragility curves. Markers indicate the points obtained applying the two simplifying assumptions described above. Table 4 shows the parameters obtained for the deterministic fragility curves.

4.3 Performance point, damage probability matrices and damage index

For a given seismic action defined by the 5% damped elastic response spectrum, there are several methods to obtain the spectral displacement that this seismic action will produce in the building defined by its capacity spectrum. Once this spectral displacement is found, fragility curves allow assessing the probabilities of exceedance of each damage state and, therefore, the probabilities of occurrence of each damage state can be easily known. In this section two well-known procedures to obtain the expected spectral displacement are applied to the selected building when submitted to the seismic actions considered. The corresponding fra-

gility curves are then used to obtain the damage probability matrices, that is, the probabilities of occurrence of each damage state. Furthermore a damage index is defined and used to represent the expected damage by means of only one parameter. The representation of this damage index as a function of the severity of the seismic action, defined in this case by the PGA, is called damage function.

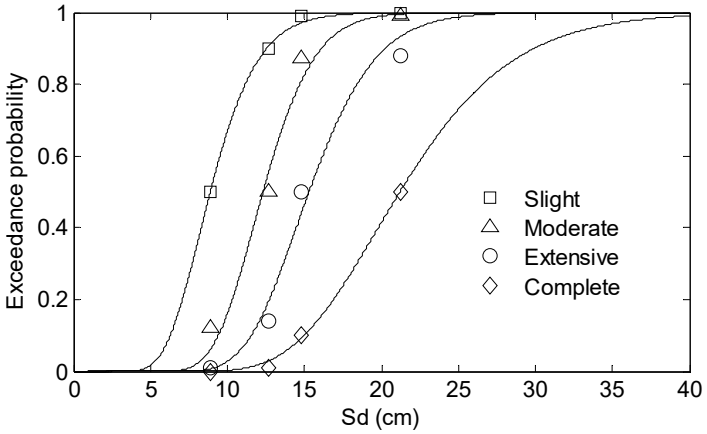

Figure 6. Deterministic fragility curves.

Table 4. Parameters, μ_{ds_i} and β_{ds_i} for the deterministic fragility curves.

	Non-null damage states			
	1) Slight	2) Moderate	3) Severe	4) Collapse
μ_{ds_i} (cm)	8.9	12.3	15.3	21.2
β_{ds_i}	0.27	0.21	0.22	0.27

4.3.1 Performance point

The performance point defines the expected spectral displacement of the building defined by its capacity spectrum when submitted to an earthquake defined by its 5% damped elastic response spectrum. There are several methods to obtain the performance point. These methods use Capacity-Demand-Diagrams that are based on inelastic response spectra in ADRS format (Mahaney *et al.* 1993, ATC 1996). Although several method improvements were proposed, see for instance Chopra and Goel (1999), for the purposes of this work two simplified methods were used. The first method is the well-known equivalent linear displacement or Equal Displacement Approximation, which assumes that the inelastic spectral displacement would be the same as if the structure would have a linear behavior. The second one, known as Pro-

cedure A in Chapter 8 of ATC-40 (ATC 1996), involves an iterative process to reduce the elastic response spectrum according to the ductility of the structure, which is calculated from the bilinear capacity spectrum. This method was rigorously tested by Fajfar (1999), who concluded that it provides a good approximation for the spectral displacement of a structure, taking into account its nonlinear behavior. In this article, these methods will be called respectively EDA and PA-8. Figure 7 a) and Figure 7 b) show an example of the application of the EDA and PA-8 methods respectively.

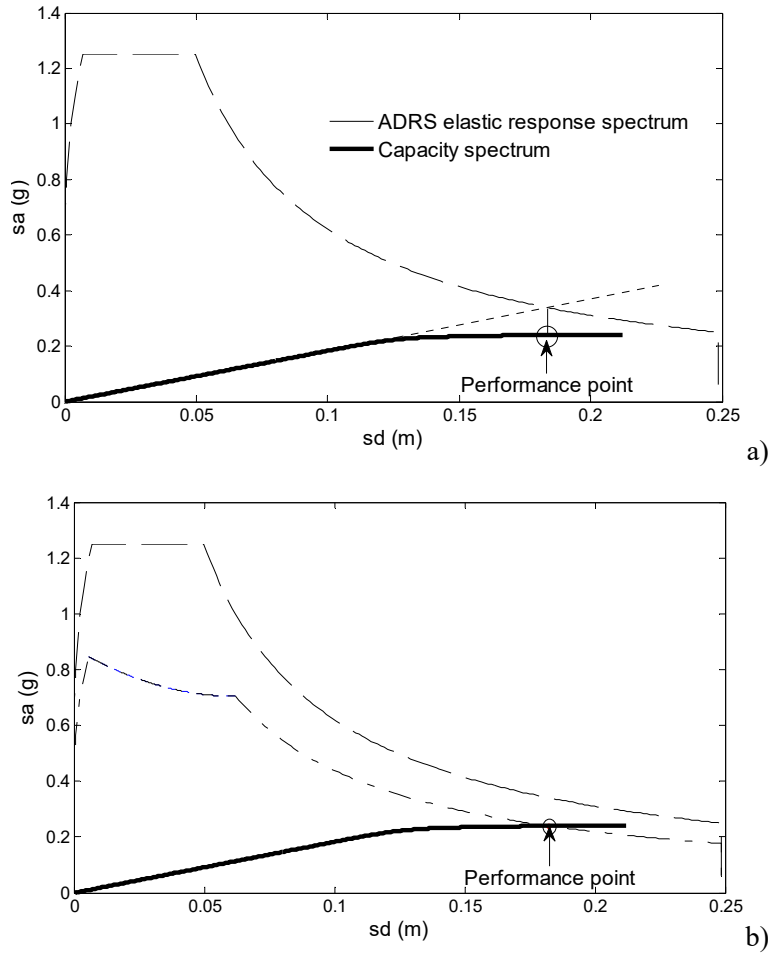

Figure 7. Example of the computation of the performance point by using the EDA (a) and the PA-8 (b) methods.

The capacity spectrum corresponds to the reinforced concrete building (Figure 5 a), while the scaled response spectrum corresponds to the EC08 2D spectrum (Figure 2). Both procedures were applied to the EC08 1A, 1D, 2A and 2D spectra and PGA values were increased between 0.01 and 1.6 g. Figure 8 shows the spectral displacements as functions of PGA for the

EDA case. Sd_p in this Figure is the spectral displacement of the performance point. Note how seismic actions compatible with 1D response spectra are the most demanding of spectral displacement, while those compatible with 2A spectra are the less demanding ones.

4.3.2 Damage probability matrices

For a given spectral displacement, *Sd,* fragility curves provide the probabilities of exceedance of the damage states. Damage Probability Matrices (DPM) are defined as the probability of occurrence of each damage state. DPM can be calculated straightforwardly from fragility curves. Should ds_i ($i = 1 \cdots 4$) be the four non-null damage states as defined above, P_i be the probability of occurrence of the damage state ds_i, and $i = 0$ correspond to the *no-damage* or *null damage* state, then $P_i(Sd)$ values can be computed in the following way:

$$\begin{aligned} P_0(Sd) &= 1 - P\left[d \geq ds_1 \middle| Sd \right] \\ P_i(Sd) &= P\left[d \geq ds_i \middle| Sd \right] - P\left[d \geq ds_{i+1} \middle| Sd \right] \quad i = 1 \cdots 3 \\ P_4(Sd) &= P\left[d \geq ds_4 \middle| Sd \right] \end{aligned} \tag{7}$$

where $P\left[d \geq ds_i \middle| Sd \right]$ values at the right side of these equations can be obtained by using Equation (5).

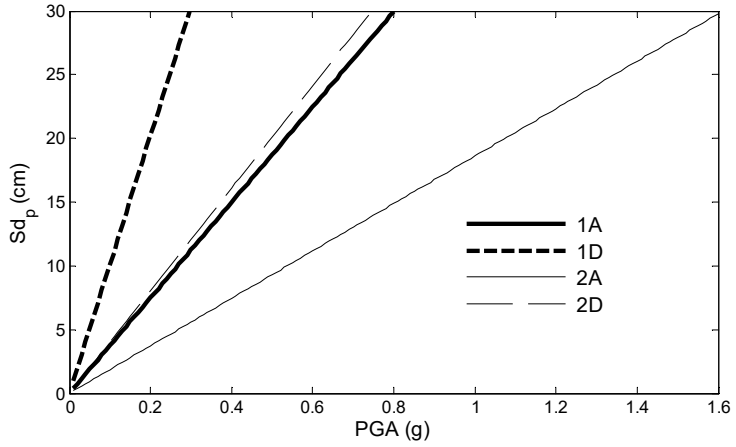

Figure 8. Spectral displacements, Sd_p, as functions of PGA for seismic actions defined by 1A, 1D, 2A and 2D EC08 response spectra. The performance points were obtained by using the EDA method. The seismic actions defined by 1D response spectrum are the most demanding of spectral displacement.

4.3.3 Damage index

It is useful to define the following damage index that can be understood as the mean damage grade.

$$di(Sd) = \sum_{i=0}^{4} iP_i(Sd) \tag{8}$$

$di(Sd)$ takes values between 0 and 4. $di(Sd) = 0$ means that the probability of the *no-damage* is equal to 1 and $di(Sd) = 4$ means that the probability of the *Complete damage* state or *Collapse* equals 1. Moreover, taking into account that the probabilities of occurrence of the damage states follow a binomial distribution, it is well known that the binomial distribution is controlled by only one parameter, taking values between 0 and 1. In our case this parameter is $DI(Sd) = \frac{di(Sd)}{4}$, being 4 the number of non-null damage states. *DI* is also known as the normalized damage index. *DI* = 0 means *no-damage* and *DI* = 1 means *collapse*. Thus $DI(Sd)$ completely defines the P_i values, and, using Equations (7), these values completely define the fragility curves. Therefore, for a given spectral displacement, these are different but equivalent ways of defining the expected damage. Furthermore, taking into account that for a given seismic action there is a relationship between Sd_p and PGA (see Figure 8), then different fragility curves and damage functions can be also represented as functions of PGA for each seismic action. That is, for each PGA, Figure 8 allows obtaining the corresponding spectral displacement Sd_p, and fragility curves (Figure 6) allow obtaining the probabilities of exceedance of each damage state. Finally the mean damage grade $DI(Sd_p)$ is obtained by using Equations (7) and (8). Figure 9 shows the damage functions for seismic actions defined by EC08 1A, 1D, 2A and 2D 5% damped response spectra. In this Figure 9 a PGA value of 0.4 g was chosen to illustrate the computation of DPM, damage indices, *di*, and the corresponding normalized damage indices, *DI*. Table 5 shows the results obtained for this case. Figure 10 displays the DPM corresponding to the values in Table 5.

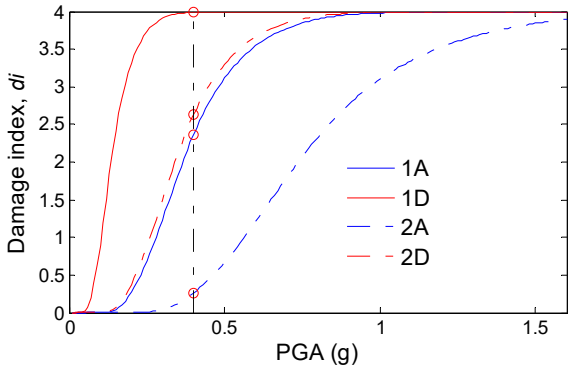

Figure 9. Damage index, *di,* as a function of PGA for seismic actions defined by 1A, 1D, 2A and 2D spectra. The fragility curves of Figure 6 and the spectral displacements of Figure 8 were used.

4.4 Nonlinear dynamic analysis

NLDA allows evaluating the response of a structure subjected to a time history of acceleration. The IDA, as proposed by Vamvatsikos & Cornell (2001) has been used in this article. The purpose here is to monitor a structural damage measure by increasing the intensity of the seismic action defined by the PGA level. Vamvatsikos & Cornell (2001) performed an interesting analogy between PA and IDA, showing how both procedures increase the loads applied to the structure and measure the response of the system in terms of a control variable, which can be the displacement at the roof or the maximum inter-storey drift, among others. Thus, IDA analysis allows also obtaining a relationship between the control variable, *Sd*, and PGA. This section describes the application of IDA as used in this work. For non-linear static analysis, Figure 8 shows that for low PGA values, the seismic inputs that produce the greatest spectral displacements are those matching the EC08 1D spectrum. For the rest of spectra, it would be necessary to scale acceleration records to large PGA values that are unlikely in Spain, where the PGA for a return period of 500 years is less than 0.25 g (NCSE-02, 2002). Therefore, in this paper, IDA is performed using only records whose response spectra are compatible with the EC08 1D spectrum.

Table 5. Damage Probability Matrices for PGA = 0.4 g. The damage index, *di,* and the normalized damage index, *DI,* are also shown.

Type of EC08 spectrum	Probabilities of the damage states					*di*	*DI*
	0) No-damage	1) Slight	2) Moderate	3) Severe	4) Collapse		
	P_0	P_1	P_2	P_3	P_4		
1A	0.03	0.15	0.36	0.36	0.10	2.36	0.59
1D	***	***	***	0.01	0.99	3.99	1.00

2A	0.74	0.25	0.01	***	***	0.26	0.07
2D	0.01	0.09	0.31	0.44	0.15	2.63	0.66

(***) means very low probability

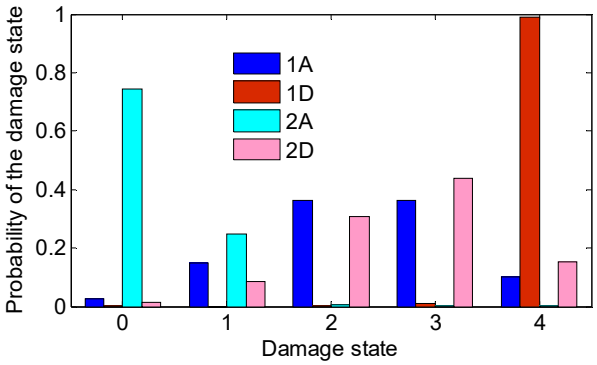

Figure 10. DPM for earthquake scenarios defined b y a PGA of 0.4 g and EC08 1A, 1D, 2A and 2D spectra. The DPM values are those in Table 5.

This limited analysis was considered sufficient for the purpose of this work. Moreover, in the nonlinear static analysis using EDA and PA-8 approaches for the EC08 1D spectrum, the PGA needed to reach the extreme case of collapse is about 0.3 g (see Figure 9). Thus, the acceleration time histories compatible with the EC08 1D spectrum were scaled from 0.06 to 0.36 g, by increments of 0.06 g. This would allow analyzing all the damage states from *null* or *no-damage* to *collapse*. In order to estimate the relationship between PGA and Sd_p, when using deterministic IDA, only one seismic record is needed. This accelerogram was obtained according to the following procedure. From the mean spectrum and its standard deviation, calculated over the 20 actual spectra that will be used in the probabilistic IDA, a characteristic spectrum is defined as that having a 5% likelihood of being exceeded. This spectrum is shown in Figure 11 a). Then, a compatible artificial accelerogram is generated after this characteristic spectrum. For the deterministic IDA, the choice of a compatible artificial accelerogram was preferred because it optimizes the matching to the target spectrum. Actual accelerograms may lead to greater misfits. The algorithm by Gasparini & Vanmarcke (1976) is used for this purpose, with the trapezoidal envelope proposed by Hou (1968). There are different ways to consider the duration of earthquakes (Hancock & Bommer 2006). In this work a simplified procedure was used. The duration of the simulated earthquake was defined as the average duration of the 20 accelerograms used in the probabilistic IDA. Figure 11 b), shows the results obtained by applying deterministic EDA, PA-8 and IDA approaches. Yielding, *Dy*,

and ultimate, *Du*, capacity spectral displacements are also plotted in this Figure. In our case, for PGA values higher than the corresponding to *Du*, the results have little or no sense. For lower PGA values simplified procedures are conservative, but there is a better agreement between spectral displacements obtained using PA-8 and IDA approaches.

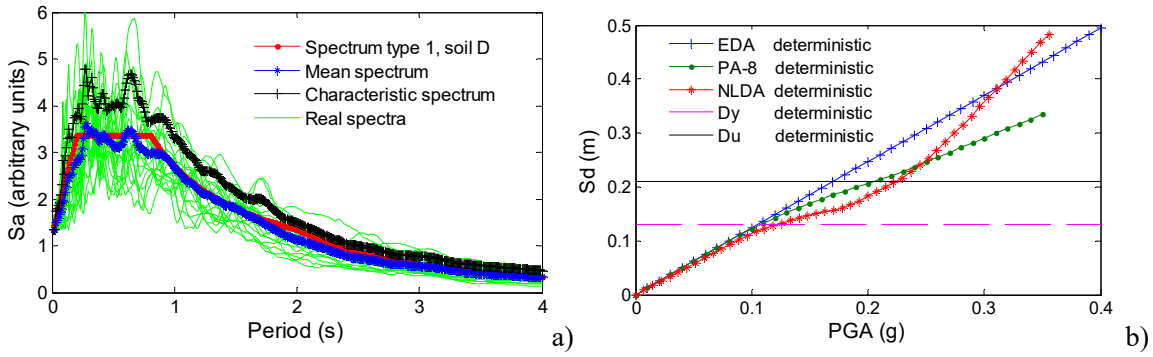

Figure 11. a) Characteristic spectrum obtained from real accelerograms. b) Results of the deterministic approach.

5 Probabilistic approach

In the previous section, the deterministic approach was used to overview several methods to assess the capacity, fragility, and expected physical damage to structures due to seismic actions. In this section this assessment is done under the assumption that the mechanical properties of materials and the seismic actions are random. Monte Carlo simulations are used to obtain probabilistic capacity and fragility curves and to assess the expected spectral displacement, by using nonlinear static and dynamic structural analyses. This way, the deterministic and probabilistic results obtained by means of simplified nonlinear static analysis can be compared to the ones obtained with more sophisticated nonlinear dynamic analysis. Furthermore, the probabilistic approach allows analyzing the influence of the variability of the input parameters into the structural response and performance of the building.

5.1 Nonlinear static analysis

PA was carried out 10 000 times, considering the random variables of the concrete compressive strength, *fc*, and the tensile strength of steel, *fy*. The values that define these random variables are shown in Table 1. The probability distributions of these random variables are assumed to be Gaussian. As described above (Figure 1), the building is composed of 56 pillars, which are divided into eight groups, each one corresponding to a storey. The correlation ma-

trix is used to take into account the correlation among the samples. Thus, high correlation is considered among the samples generated for the pillars belonging to a same group. But, the correlation among the samples generated for pillars of different groups is considered to be null. Therefore, a kind of spatial variability of the randomness is also taken into account. The same approach is used with the beams of equivalent inertia, which model the waffle slabs. The pillars are attached to waffle slabs that are modeled by beams having an equivalent inertia. Since the floors are alike at all levels, there is only one type of cross section for these beams. In each iteration of the Monte Carlo technique, for each element, pillar or beam, of one group, a random sample of concrete strength and steel is generated, according to the procedure described in Kalos & Whitlock (1986). Thus, in every implementation of PA, the resistance of structural elements varies in a stochastic way. Figure 12 shows the 10 000 capacity curves, the mean capacity curve and the deterministic capacity curve, which were obtained using the characteristic strength values. It is worth noting that the maximum displacement value of the curve obtained using characteristic strength values is exceeded by 82.5% of all the capacity curves. Therefore, the probability of the structure reaching collapse before this value is 17.5%. Furthermore, key parameters of the capacity curves coming from the Monte Carlo simulations are also random. Figure 13 shows the correlation plots between the initial stiffness, *Ko*, and *fc,* and between the ultimate capacity displacement, $\underline{\delta_u}$, and *fy*. It can be seen how δ_u slightly increases with *fy* (Figure 13 a). Figure 13 b shows the strong dependence between *Ko* and the compressive strength of concrete, *fc*. In order to have a more accurate measure of the degree of dependence between input and output variables, the correlation matrix was calculated. The input random variables are *fy* and *fc.*

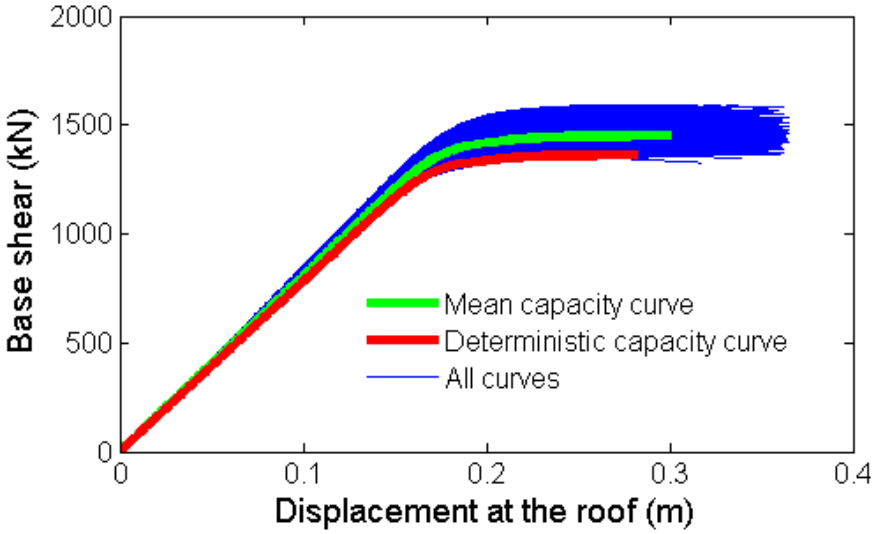

Figure 12. Capacity curves obtained from the probabilistic approach, mean capacity curve and capacity curve obtained with the deterministic approach by using characteristic values.

The output random variables considered herein are the stiffness of the elastic section of the capacity curve, known as *Ko*, the yielding and ultimate spectral displacements of the bilinear form of the capacity spectrum, namely *Dy* and *Du,* and the ductility capacity factor, *q*, which can be estimated by using the following equation:

$$q = \frac{Du}{Dy} \tag{9}$$

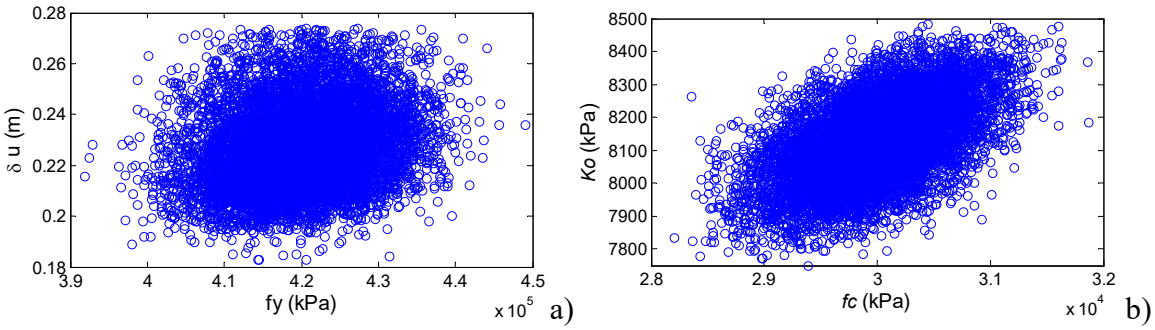

Figure 13. Correlation between the ultimate displacement, δ_u, of the capacity curve and *fy* (a) and between *Ko* and *fc* (b).

Once the input and output random variables are defined, the correlation matrix ρ_{ij} can be calculated using the following equation:

$$\rho_{ij} = \frac{Cov(x_i, x_j)}{\sigma_{x_i}\sigma_{x_j}} \tag{10}$$

where x_i and x_j are variables, *Cov* is their covariance, and σ_{x_i} and σ_{x_j} are the standard deviations of the variables x_i and x_j. The correlation matrix among the random variables considered is shown in Table 6.

Table 6. Correlation matrix between the random variables

		Input variables		Output variables			
		fy	*fc*	*q*	*Ko*	*Dy*	*Du*
Input variables	*fy*	1.00	0.00	0.13	-0.01	0.34	0.21
	fc	0.00	1.00	-0.14	**0.55**	0.18	-0.10
Output variables	*q*	0.13	-0.14	1.00	-0.48	-0.20	**0.97**
	Ko	-0.01	**0.55**	-0.48	1.00	**0.71**	-0.33
	Dy	0.34	0.18	-0.20	**0.71**	1.00	0.03
	Du	0.21	-0.10	**0.97**	-0.32	0.03	1.00

As expected, a strong correlation value of 0.71 exists between stiffness and yielding spectral displacement, and a value of 0.97, between ductility and ultimate spectral displacement. Additionally a significant correlation value of 0.55, between *Ko* and *fc,* and of 0.34, between *fy* and *Dy,* can be observed. The correlation matrix shows the wealth of information that can be obtained from probabilistic approaches.

5.2 Fragility curves

As seen above, simplified procedures may be used to obtain fragility curves from bilinear capacity spectra, which can be easily derived from capacity spectra. So, Equations (6) allow computing the damage states thresholds for each one of the capacity curves of Figure 12. Figure 14 shows these damage states thresholds (ds_i), together with those corresponding to the deterministic capacity curve. Table 7 shows the mean values, μ_{ds_i}, standard deviations, σ_{ds_i}, and coefficients of variation, *c.o.v*. The deterministic damage state thresholds, $ds_{i,\det}$, are also shown in Table 7 and in Figure 14. It can be observed in this figure that ds_1 and ds_2 thresholds are strongly correlated with spectral acceleration because the corresponding spectral displacements are near the zone where the behavior of the building is linear. However, ds_3 and especially ds_4, thresholds exhibit much more dispersion. Note that the dispersion,

and thus the probability of occurrence of ds_i inferior to $ds_{i,\det}$, increases as spectral displacements augment. Table 8 shows the probability of ds_i being inferior to $ds_{i,\det}$. Each fragility curve is completely defined should ds_i and β_{ds_i} be known. As explained above these parameters can easily be estimated from capacity spectra and simplifying assumptions.

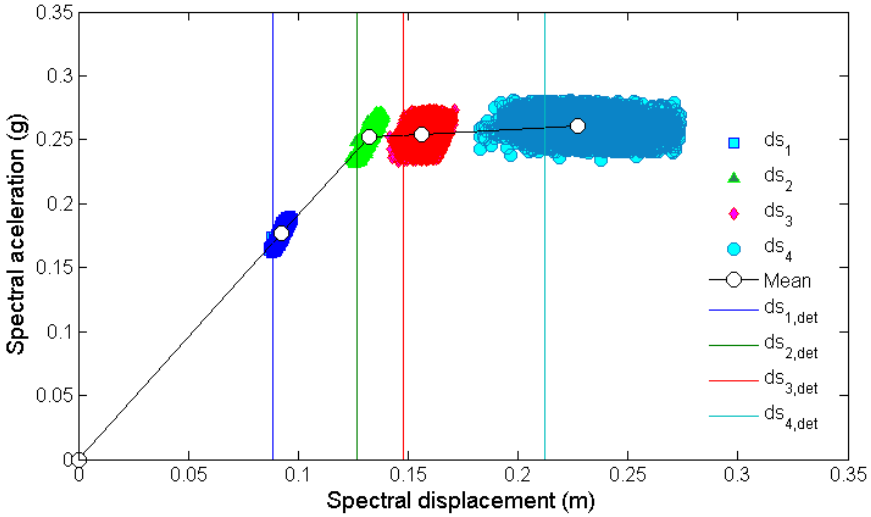

Figure 14. Damage states thresholds obtained with the probabilistic and deterministic approaches.

Table 7. Mean values, standard deviations and coefficients of variation *c.o.v.* of the damage state thresholds. Deterministic values are also included.

	Damage states			
	1) Slight	2) Moderate	3) Extensive	4) Collapse
Mean values μ_{ds_i} (cm)	9.2	13.2	15.6	22.7
Standard deviations σ_{ds_i} (cm)	0.16	0.22	0.51	1.60
Coefficients of variation *c.o.v*	0.02	0.02	0.03	0.07
Deterministic values $\mu_{ds_{i,Det}}$ (cm)	8.8	12.7	14.8	21.2

Table 8. Probability that the thresholds of the damage states, obtained with the probabilistic method, be less than the ones estimated by the deterministic procedure.

$P[ds_1 < ds_{1,\det}]$	$P[ds_2 < ds_{2,\det}]$	$P[ds_3 < ds_{3,\det}]$	$P[ds_4 < ds_{4,\det}]$
0.004	0.004	0.029	0.175

Figure 15 a) shows the fragility curves. Again, the variability increases with increasing damage states. Note that this increment is due to the increasing nonlinearity of the structural re-

sponse. Figure 15 b) plots the mean ds_i values of the lognormal function against the corresponding β_{ds_i}, thus illustrating the correlation between ds_i and β_{ds_i}. Table 9 shows the correlation coefficients, which also augment as ds_i increases. In order to represent the probabilistic fragility curves in a parametric form, a Gaussian model for the parameters describing the fragility curves was tested. Figure 16 a) and b) compare the empirical and parametric models, respectively for ds_i and β_{ds_i}, showing a good fit.

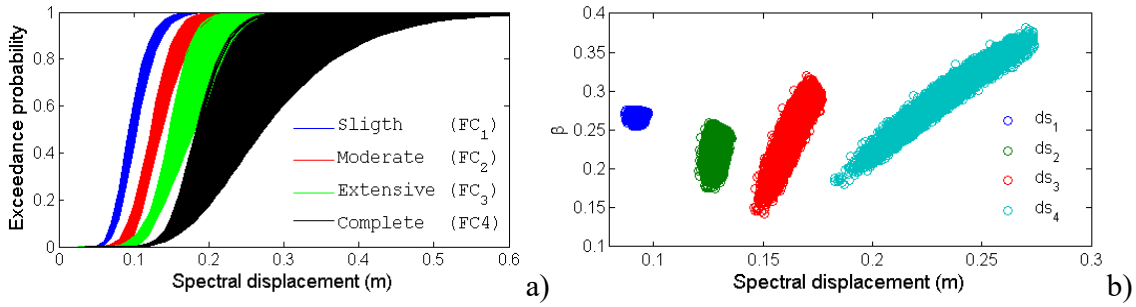

Figure 15 Fragility curves obtained with the probabilistic approach (a), and correlation among parameters ds_i and β_{ds_i}, which define the lognormal functions of the fragility curves (b).

Table 9. Correlation coefficients between ds_i and β_{ds_i}

	ds_1 - β_{ds_1}	ds_2 - β_{ds_2}	ds_3 - β_{ds_3}	ds_4 - β_{ds_4}
ρ_{ij}	-0.20	-0.20	0.82	0.97

Table 10 presents the mean values and standard deviations of the Gaussian models. The coefficients of variation are also shown in this table.

Table 10. Mean values, μ, standard deviations, σ, and coefficients of variation, *c.o.v.*, of the random variables that define the fragility curves for the four non-null damage states.

	Damage states							
	1) Slight		2) Moderate		3) Extensive		4) Complete	
	ds_1 (cm)	β_{ds_1}	ds_2 (cm)	β_{ds_2}	ds_3 (cm)	β_{ds_3}	ds_4 (cm)	β_{ds_4}
μ	9.2	0.27	12.8	0.218	16.1	0.231	22.7	0.28
σ	0.2	0.004	0.2	0.015	0.5	0.03	1.6	0.035
c.o.v.	0.022	0.015	0.016	0.069	0.031	0.130	0.070	0.125

Thus, it is possible to estimate these parameters, and consequently the fragility curves, for any confidence level. Another equivalent way of analyzing the results of the Monte Carlo simulation is the following: for each spectral displacement and for each set of fragility curves

in Figure 15 a), the mean value, 95% confidence level and standard deviation is obtained. Figure 17 a) shows the mean and the 95% confidence level fragility curves, together with the deterministic fragility curves. Figure 17 b) shows the standard deviation of each fragility curve as a function of the spectral displacement. It is worth noting that the 95% confidence level fragility curves are greater than the deterministic ones. The difference between these curves augments with increasing damage states and at intermediate spectral displacements close to the damage states thresholds. Note also in Figure 17 b) that, for each damage state, the greatest standard deviations of the fragility curves, and thus the greatest uncertainties, occur around damage states thresholds, namely around the mean values of the lognormal distributions. Again these uncertainties augment with increasing spectral displacements. As it has been pointed out above, this fact is due to the increase of the nonlinear response of the building at increasing seismic actions.

5.3 Performance point and damage index

In order to compare the nonlinear static and dynamic results, as the IDA scheme has been adopted, it is necessary to obtain the relationship between PGA and spectral displacement, Sd_p, for increasing seismic actions. So, in this section the static probabilistic approach is applied to obtain the performance spectral displacements expected as a function of PGA. Thus, for each of the four spectra considered and for each of the 10 000 capacity curves, the methods to obtain the performance point described above were applied. Therefore, in order to compare the static and dynamic results, the spectra of actual accelerograms, compatible with the selected EC08 spectra, were used for the static-based-methods. As for the case of EDA procedure, it is worth noting that, since the result is linear, it is sufficient to scale the response spectra for a single PGA. Therefore, it suffices to extend a line from the origin passing through this point. Figure 18 shows an example of the 5% damped elastic response spectrum compatible with EC08 1D spectrum. As it can be seen in Figure 18, these response spectra in ADRS format are not one-to-one functions, as they show an irregular shape. This fact complicates the automation of the iterative process, which is easier to apply in case of smoothed spectra, usually defined by simple piecewise analytical functions.

5.3.1 Performance point

The main results obtained with the probabilistic EDA and PA-8 methods are summarized in Figure 19.Figure 19 a) shows the mean spectral displacements for the four EC08 spectra considered, and the corresponding standard deviations. EDA results are conservative; close to safety, since the assumptions, underlying EDA technique, never underestimate the expected spectral displacement. Again, dispersion augments with increasing PGA and, consequently, with increasing spectral displacements. This means that, in probabilistic approaches, it is necessary to assess the uncertainty of this relationship as a function of PGA, as the $Sd_p(PGA)$ functions of Figure 19 a) are crucial for damage assessment. A nice measure of this uncertainty can be, for instance, the standard deviation (see Figure 19 b).

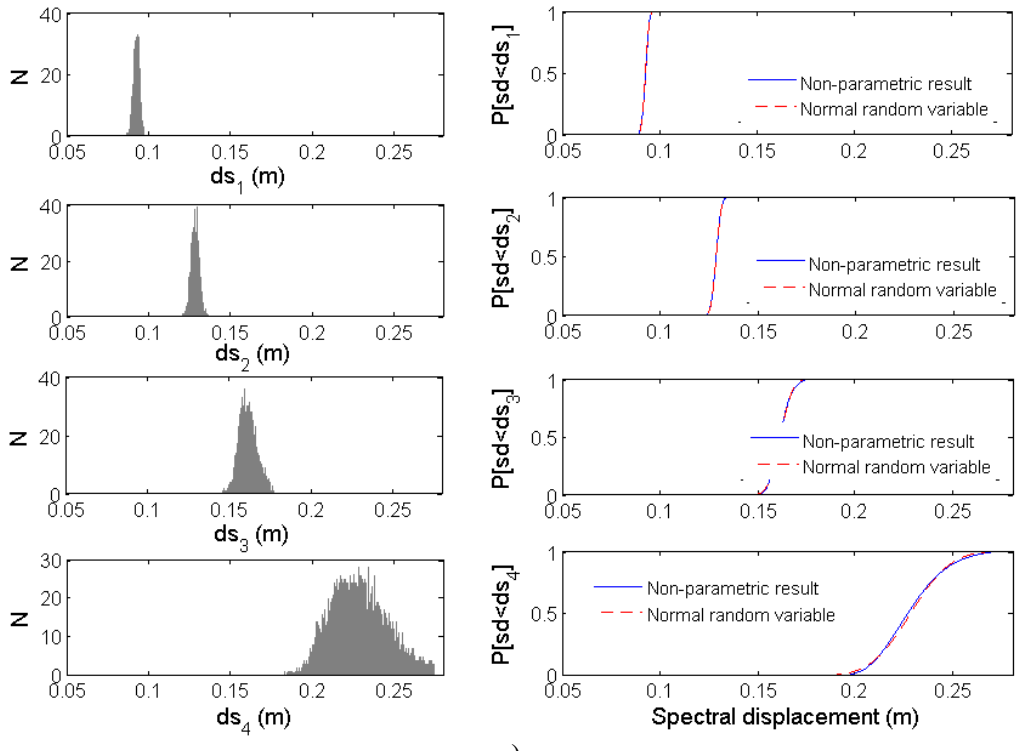

a)

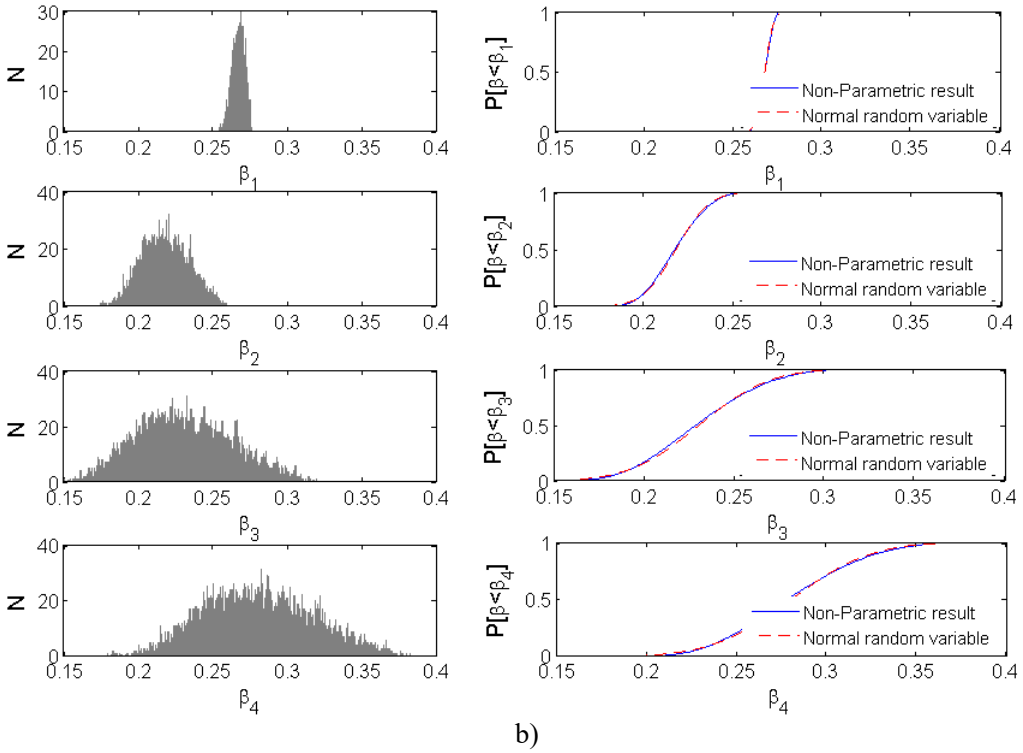

Figure 16. Histograms and comparison with Gaussian random distributions for ds_i (a), and β_{ds_i} (b).

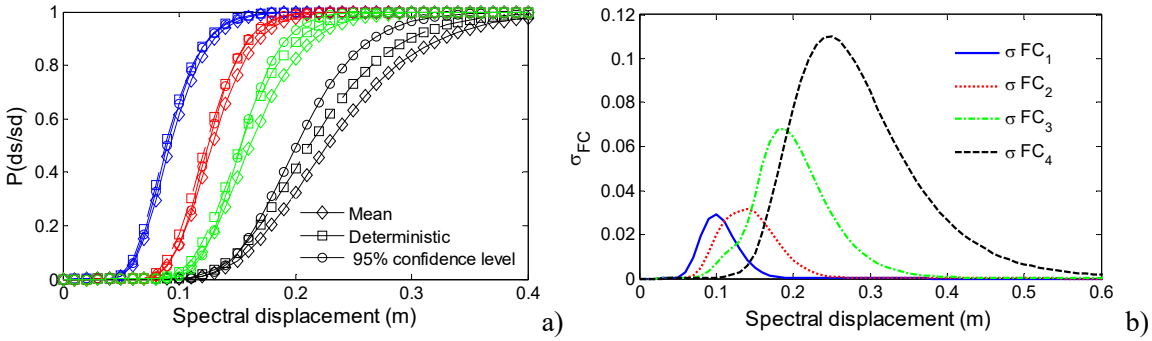

Figure 17. Fragility curves obtained with the probabilistic and deterministic approaches. The 95% confidence level fragility curves are also shown (a). Standard deviation of the probabilistic fragility curves (b).

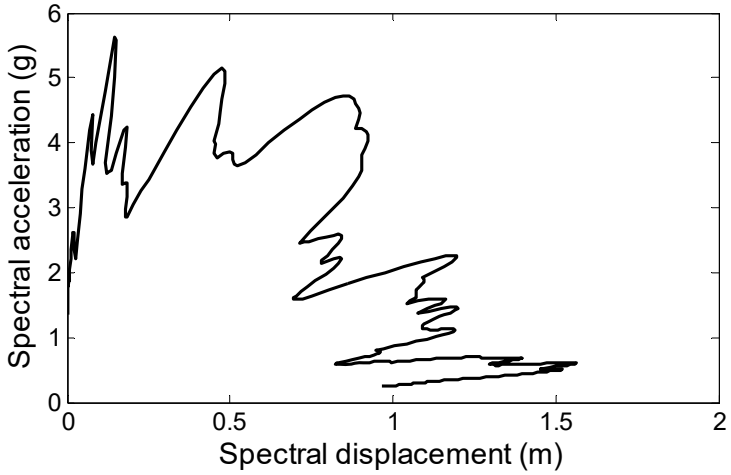

Figure 18. Example of a 5% damped elastic response spectrum in ADRS format for an accelerogram matching the EC08 1D response spectrum.

This effect, due to increasing uncertainties, is more important for severe earthquakes and when high confidence levels are needed. On the other hand, the standard deviations of the EC08 2A spectrum are higher than the ones of the EC08 1D spectrum.

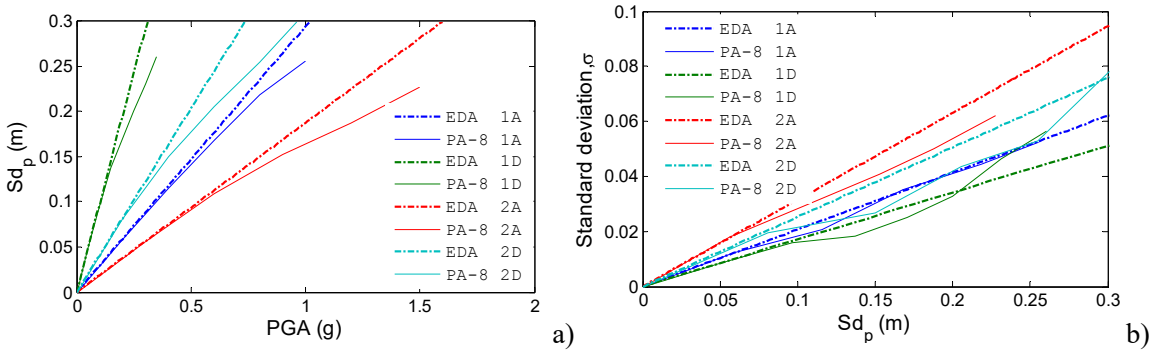

Figure 19. a) Comparison of spectral displacements, Sd_p obtained with probabilistic EDA and PA-8 techniques. b) Comparison of the corresponding standard deviations.

For the EC08 1D spectrum and PA-8 method a significant increase of the uncertainties can be observed for high spectral displacements.

5.3.2 Damage index

Concerning the expected damage, only the case of the EC08 1D spectrum is analyzed here, as this is the most demanding case and will be used for comparison with the IDA probabilistic results. Thus, only the corresponding mean spectral displacements for the EDA and PA-8 techniques are used (see Figure 19 a). Figure 20 a) compares the *DI* obtained by means of the

EDA approach and using mean fragility curves, 95% confidence level fragility curves and the deterministic approach using characteristic values. Figure 20 b) corresponds to the PA-8 approach. Observe how, for the building here analyzed, the deterministic approach, by using characteristic values, is a fairly good approach. However, especially for high PGA values, the expected deterministic damage indexes can be slightly lower than the ones corresponding to the 95% confidence level obtained with the probabilistic approach. Therefore, the use of characteristic values does not guarantee that the output variables will have the same confidence level than the input ones. Furthermore, as shown in Figure 19 b), significant dispersion is expected.

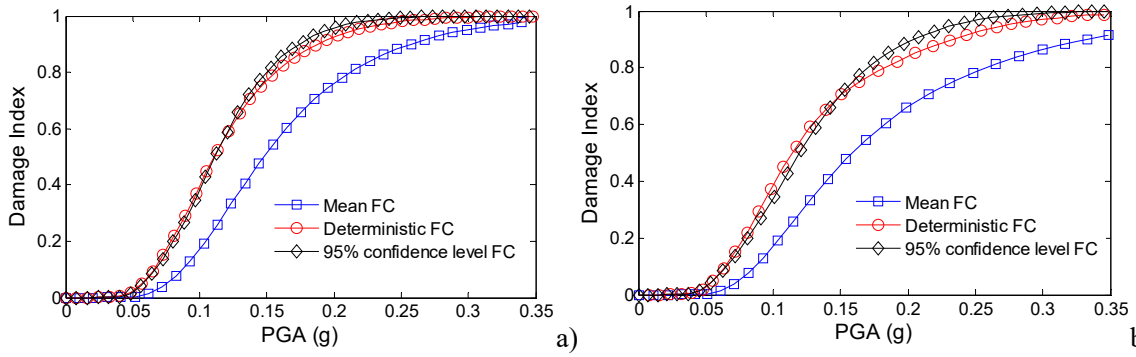

Figure 20. Damage index functions by using EC08 1D spectrum: EDA procedure a), and PA-8 procedure b). In both cases Mean, deterministic and 95% confidence level fragility curves (FC) were used to assess the damage index.

5.4 Nonlinear dynamic analysis

As in the deterministic NLDA, the IDA procedure was used, but the probabilistic approach was performed considering the mechanical properties of materials and seismic action as random variables. The twenty accelerograms compatible with the EC08 1D spectrum were scaled, by increments of 0.06 g, until reaching the value of 0.36 g, thus allowing the analysis of a wide range of spectral displacements covering all the damage states from *null* or *no-damage* to *complete* or *collapse* damage states. However, for each of the 20 records, only 100 samples of the mechanical properties were generated. This number of samples was considered sufficient for the probabilistic analysis as this implies 2 000 NLDA for each of the 6 PGA considered in the IDA, which would render a total of 12 000 NLDA. Figure 21 a) shows the results obtained. Each color in Figure 21 corresponds to a PGA value. For each color, namely for each PGA value, 20 clouds, having 100 points each cloud, can be observed. So, each cloud corresponds to a real accelerogram and each one of the 100 points of each cloud

corresponds to a random value of the mechanical properties of the materials. This figure illustrates one of the most important results of this work, clearly showing the influence of the randomness of real seismic actions on the uncertainties of the response of the building. Note how the maximum displacement at the roof and the shear at the base augments as PGA's increase, as well as how the dispersions, and indeed the uncertainties, increase too. Should the results corresponding to a PGA equal to 0.06 g be closely observed (Figure 21 b), the 20 clouds associated to the 20 accelerograms can be clearly distinguished. For each cloud, the differences are due to the variability of the strength properties of the materials. Nevertheless, the differences among different clouds are due to the variability of the 20 accelerograms used for the same PGA and EC08 1D spectrum, thus indicating that an important source of randomness is the seismic action. Similar comments can be said for all 6 PGA values. However, it can be also seen in Figure 21 a) that as PGA increases, the overall dispersion augments, being more and more difficult to distinguish the different clouds corresponding to the different accelerograms. However, the influence of the variability of the seismic action is also predominant. Figure 21 c) shows the detail for the extreme case of PGA = 0.36 g. This fact is attributed to the growth of the influence of the variability of the mechanical properties of the materials on intense seismic actions as the behavior of the building is governed by the nonlinear response. Consequently, the quantitative observation of the great influence of the variability of the seismic actions, and that of the variability of the properties of the materials with increasing PGA's, are important outcomes of this work. The influence of ground-motion variability in damage and risk calculations has also been described and discussed in Bommer & Crowley (2006). In order to estimate the expected damage, the spectral displacements were computed as a function of PGA. Figure 22 a) shows this function. In this Figure the yielding, *Dy*, and ultimate, *Du*, displacements, together with their 95% confidence intervals, were also depicted. Figure 22 b) shows the standard deviations of the spectral displacements. Again the standard deviations augment with increasing spectral displacements. Figure 23 shows the expected damage index as a function of PGA. Mean and 95% confidence curves are plotted together with the deterministic case.

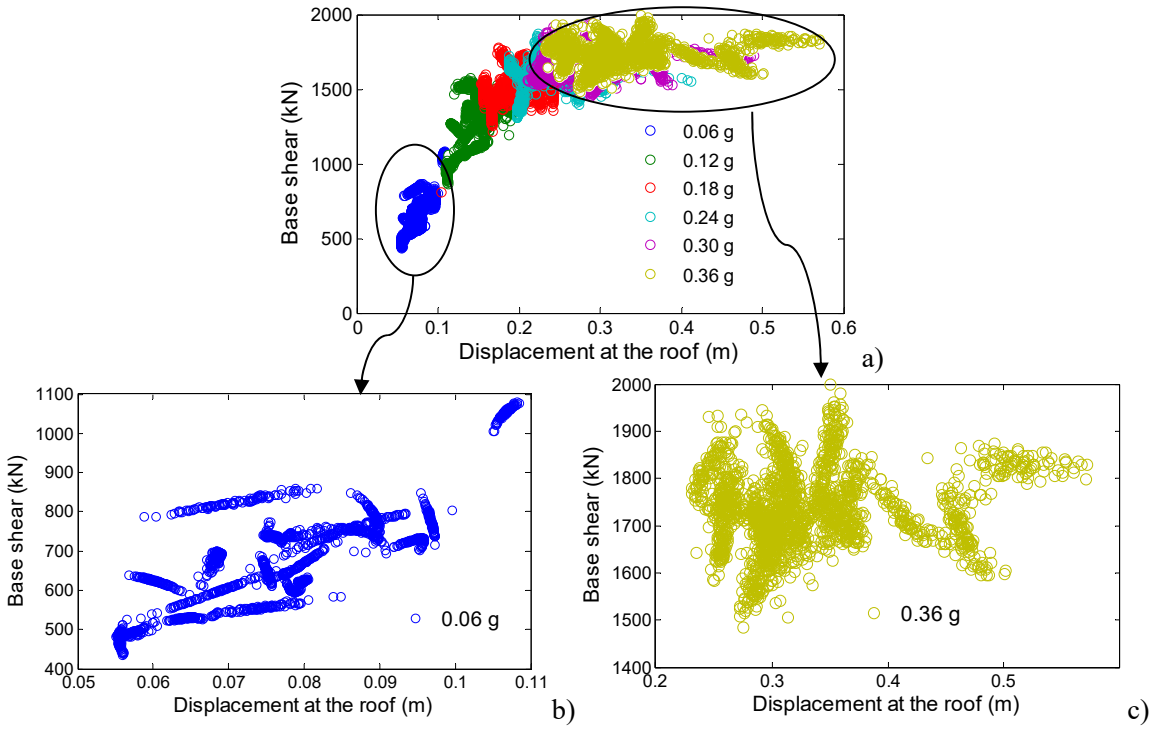

Figure 21. Overall results of probabilistic NLDA, a), and details of the cases of PGA = 0.06 g, b), and PGA = 0.36 g c).

For intermediate PGA values the expected damage index with a 95% confidence level is greater than the corresponding to the deterministic case, in which characteristic values are used. Figure 23 is similar to Figure 20, where the probabilistic results of applying EDA and PA-8 procedures are illustrated. These three cases, EDA, PA-8 and IDA, will be shown together, compared and discussed in the following section.

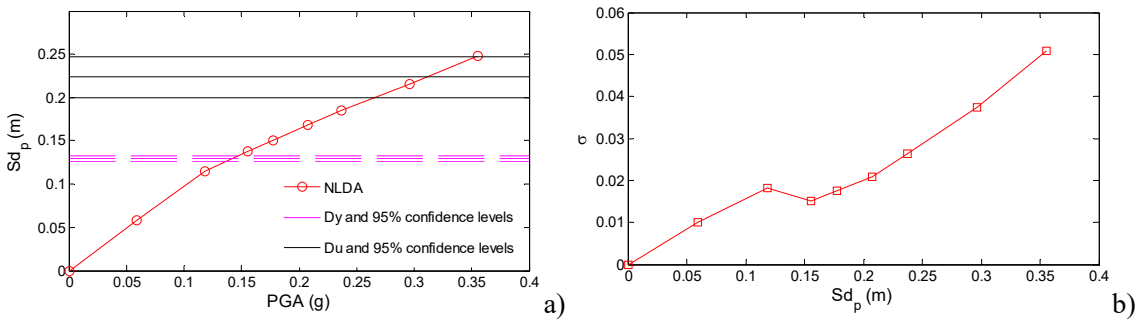

Figure 22. a) Relationship between the PGA and the mean spectral displacement obtained with IDA. The 95% confidence intervals for the spectral displacements of the yielding and ultimate capacity points are also shown. b) Corresponding standard deviations.

6 Discussion and conclusions

In this section the most relevant results of the probabilistic approach are compared and discussed and the main conclusions of this work are outlined. Moreover, an example of the practical use of probabilistic techniques to assess the expected seismic damage and risk of actual buildings is presented and discussed.

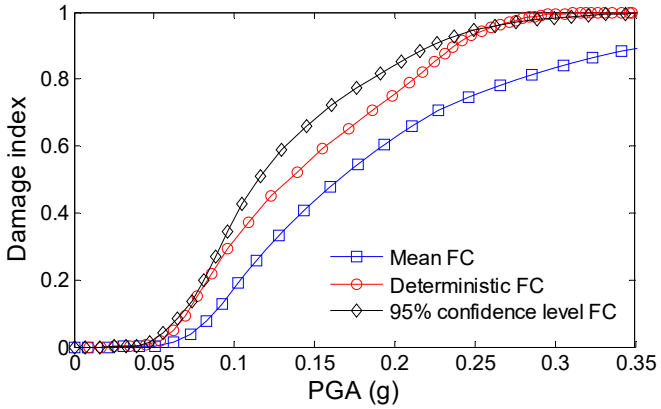

Figure 23. Damage index function by using EC08 1D spectrum and NLDA procedure, Mean, deterministic and 95% confidence level fragility curves (FC) were used to assess the damage indices.

6.1 Comparison of the static and dynamic probabilistic approaches

Figure 24 summarizes the $PGA(Sd_p)$ functions obtained by means of the EDA, PA-8 and IDA probabilistic procedures. Figure 24 a) shows the mean values obtained and Figure 24 b) shows the corresponding standard deviations. For comparison purposes, Figure 24 a) also shows the yielding, *Dy*, and the ultimate, *Du*, spectral displacements together with their 95% confidence intervals. In both Figures, but particularly in Figure 24 b), significant changes in the slopes of the PA-8 and IDA curves can be observed. These changes begin just close to the yielding displacement, *Dy*, and they are attributed to changes in the behavior of the structure when entering the nonlinear part of the capacity spectrum, which also corresponds to the nonlinear dynamic response (Vargas *et al.* 2010). It can be seen that EDA and PA-8 simplified approaches do not underestimate the spectral displacement, when these simplified approaches are compared to the more realistic IDA procedure. Nevertheless PA-8 technique gives a more accurate estimation of the spectral displacement than EDA. Moreover, the greatest standard deviations correspond to the highest spectral displacements, around and over the ultimate capacity displacement, *Du*. Concerning expected damage, Figure 25 summarizes the results

of the damage index, *DI*, as a function of the PGA. In this Figure, the median spectral displacements, Sd_p, of the ordinates of the graph of Figure 24 a) are used together with the corresponding fragility curves at the 95% confidence level. PA-8 and NLDA provide similar results, but, although somewhat conservative in the range between PGA values of 0.12 and 0.28 g, EDA never underestimates the expected damage.

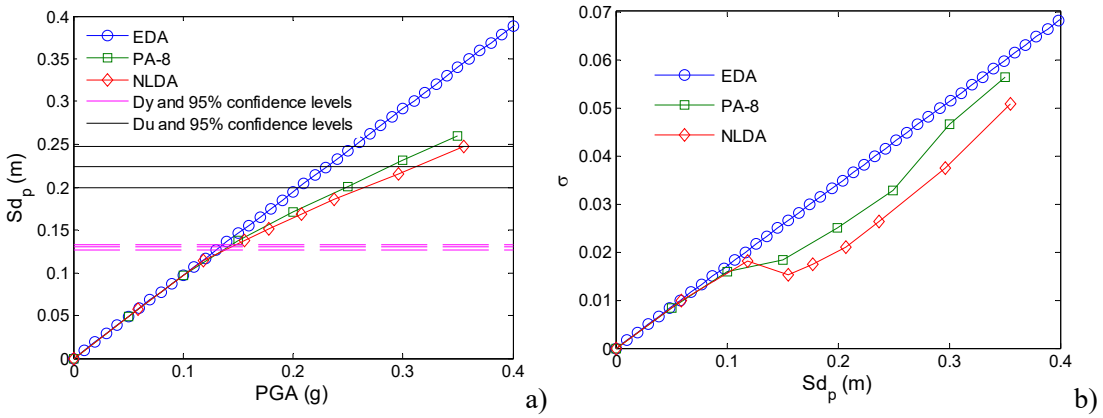

Figure 24. Relationship between the PGA and the median spectral displacement, Sd_p, obtained with EDA, PA-8 and NLDA. The 95% confidence intervals for the yielding, *Dy*, and ultimate, *Du*, spectral displacements are also plotted a). Corresponding standard deviations b).

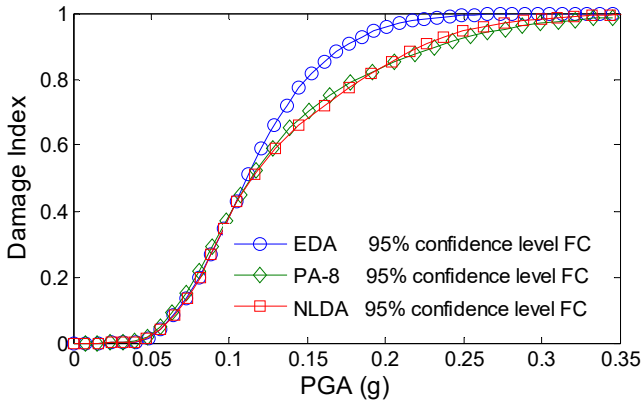

Figure 25. Damage index as a function of the PGA obtained for the EDA, PA-8 and IDA probabilistic methods. Median spectral displacements, Sd_p, and 95% confidence fragility curves were used.

The corresponding spectral displacements 0.12 and 0.23 m are close to the thresholds of *Moderate* and *Complete* damage states (see Figure 14 and Table 7). The main cause of this effect is attributed to the fact that EDA procedure does not capture the nonlinear behavior of the building.

6.2 Applicability of the probabilistic approach

As stated above, most of the seismic risk assessments carried out up to now in urban areas were performed using deterministic approaches. The results of these works are usually understood as mean or median expected values. In this section we discuss about the influence that the randomness of the strength properties of the materials, steel and concrete, and the randomness of the seismic action have in the randomness of the expected damage. Moreover, two specific scenarios are analyzed in order to illustrate how the probabilistic results should be understood and how they can be used in practical applications. To do that, Monte Carlo simulations were performed first, separating the randomness of the mechanical properties of the materials from that of the seismic actions. Figure 26 shows the standard deviation of the expected spectral displacement as a function of PGA in the following three cases: 1) only the mechanical properties of the materials are assumed to be random, while the seismic action is assumed to be deterministic, 2) only the seismic action is assumed to be random, while the mechanical properties of the materials are assumed to be deterministic and 3) both, the properties of the materials and the seismic action are assumed to be random. These three cases are analyzed using NLDA. Note how the influence of the uncertainties of the mechanical properties of the materials is very low compared to the influence of the uncertainties of the seismic actions. Uncertainties of the seismic action may have been overestimated due to the insufficiency of the accelerogram databases used in this study. Probably these uncertainties can be decreased by using larger and more specific databases. So, in risk assessment studies the uncertainties of the involved parameters should be carefully addressed. One possibility is, for instance, to use logical trees with different reasonable assumptions and weightings in a similar way to that used in probabilistic seismic hazard analyses (PSHA).

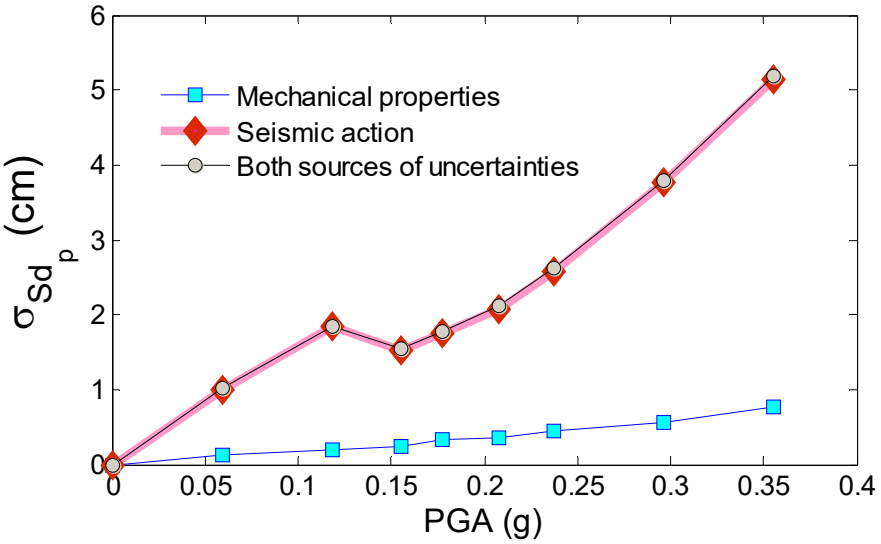

Figure 26. Standard deviation, σ, of the spectral displacement, Sd_p, as a function of PGA, considering the randomness of the mechanical properties of the materials (concrete and steel), the randomness of the seismic actions and both uncertainties.

It is worth noting that the standard deviations corresponding to the case in which both uncertainties are taken into account can be easily obtained from the quadratic composition of standard deviations, that is:

$$\sigma_T \cong \sigma_Q = \sqrt{\sigma_M^2 + \sigma_A^2} \tag{11}$$

where σ_T is the standard deviation taking into account both uncertainties, σ_M corresponds to the mechanical properties, σ_A corresponds to the seismic action, and σ_Q is the quadratic composition of σ_M and σ_A. Table 11 shows selected values of PGA and the corresponding standard deviations taken from Figure 26. In this table the standard deviations are compared to the quadratic composition according to Equation (11). This result confirms that the seismic actions and the mechanical properties of the materials are independent random variables.

Table 11. Standard deviations in Figure 26 for PGA values of 0.18, 0.24 and 0.36 g. σ_M, σ_A and σ_T are respectively standard deviations corresponding to mechanical properties, seismic actions and both types of uncertainties. σ_Q is the quadratic composition of σ_M and σ_A, according to Equation (11).

PGA (g)	σ_M (cm)	σ_A (cm)	σ_T (cm)	σ_Q (cm)
0.18	0.32	1.74	1.77	1.77
0.24	0.45	2.58	2.62	2.62
0.36	0.76	5.13	5.19	5.19

In order to illustrate the usefulness of the probabilistic approach, two hypothetical earthquake scenarios are then considered. Figure 27 shows the spectral displacement of the performance points, Sd_p, as a function of PGA. The median values and the 95% confidence levels are illustrated in this figure.

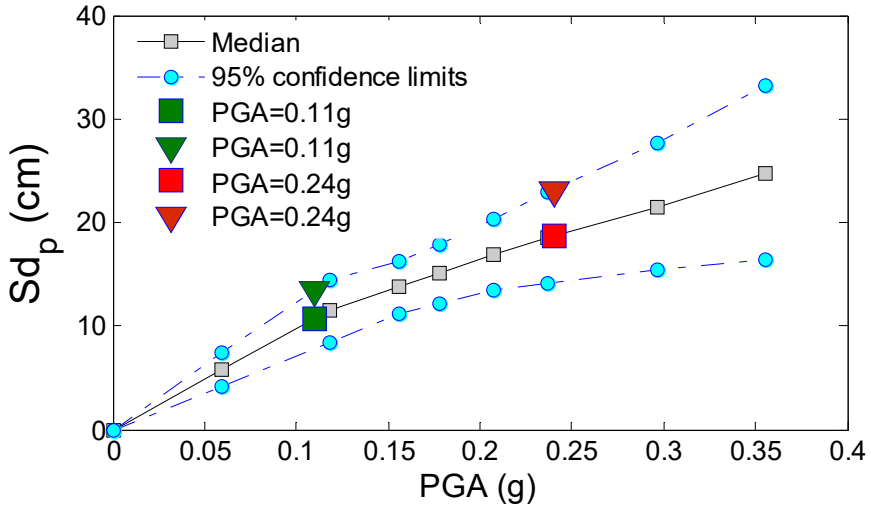

Figure 27. *$Sd_p(PGA)$* function defining the expected spectral displacement as a function of PGA. Median and 95% confidence level curves are shown. Two earthquake scenarios defined by PGA values of 0.11 and 0.24 g are also depicted.

The first scenario corresponds to a relatively low demand earthquake defined by a PGA value of 0.11g; the second one corresponds to a relatively highly demanding earthquake, defined by a PGA value of 0.24 g. Both scenarios are also depicted in Figure 27. To avoid considering the uncertainties twice, in practical applications, special care must be taken. So, to estimate the expected damage one of the procedures described below can be followed. **Procedure A:** the function defining the expected performance spectral displacement as a function of PGA, *$Sd_p(PGA)$*, is assumed to be probabilistic and the fragility curves are assumed to be deterministic; so, for a given PGA the spectral displacement of the performance point is obtained varying randomly the seismic actions and the mechanical properties together. **Procedure B**: fragility curves are assumed to be probabilistic as well as the function *$Sd_p(PGA)$* In **Procedure A** the uncertainties of the seismic actions and of the mechanical properties of the materials, are included in the *$Sd_p(PGA)$* function (see Figure 27). In **Procedure B** the uncertainties in the mechanical properties of the materials are considered in the construction of the fragility curves, while the uncertainties in the seismic actions are considered in the construction of the *$Sd_p(PGA$*) function. Therefore the *DI(PGA)* function relating the expected damage and *PGA*

takes into account both sources of uncertainty; in this case the standard errors of the *DI(PGA)* can be obtained from the quadratic composition of the standard errors coming from the fragility curves and from the $Sd_p(PGA)$ function. **Procedure A** is used in the following as an application example. For each of the two earthquake scenarios, the expected spectral displacements are taken from the curves $Sd_p(PGA)$ in Figure 27 considering median and upper 95% confidence values. The corresponding numerical values are shown in Table 12. Figure 28 shows the $DI(Sd_p)$ curve. This $DI(Sd_p)$ function was obtained using median fragility curves and median seismic actions, and it is assumed to be deterministic. The median and 95% upper confidence level spectral displacements of the performance point, Sd_p. obtained in Figure 27, are then used to get the corresponding expected damage indices. Finally, the assumption of the binomial distribution of the probabilities of damage states allows computing these important probabilities. Table 12 summarizes the obtained results and Figure 29 shows the corresponding expected damage probability matrices. Thus the probabilistic approach allows obtaining results for all confidence levels and it produces information that is richer and more useful for civil protection stakeholders and decision makers, who may establish and choose the preferred levels of security.

As a special case, please note in Table 12 and in Figure 29 how for the 0.24 g earthquake scenario the median and the 95% confidence level probabilities of the *Complete* damage state (ds_4) are respectively of 28% and 56%.

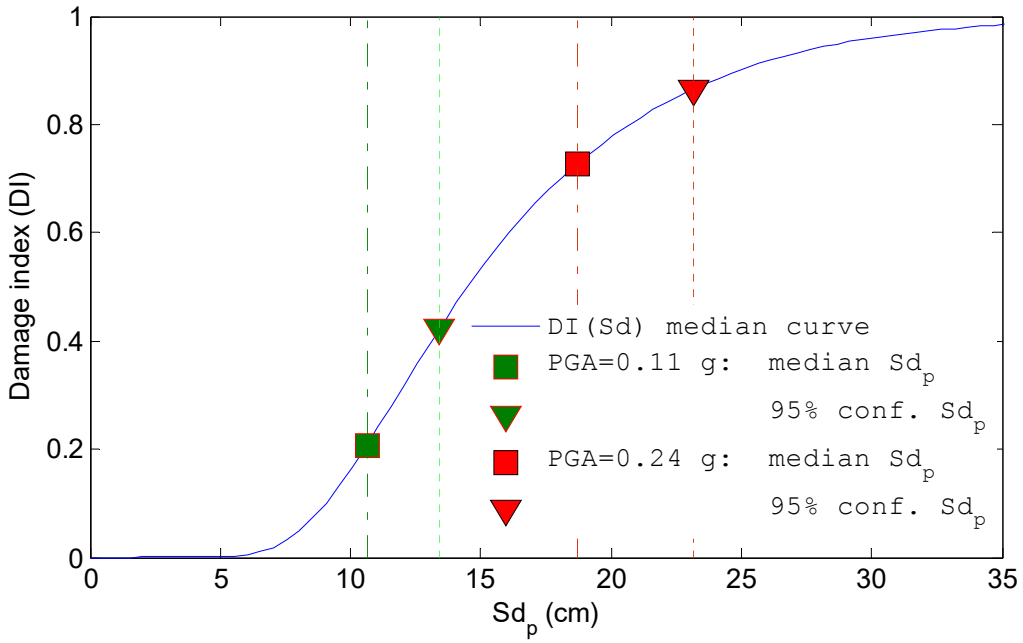

Figure 28. *DI(Sd$_p$)* function defining damage index, *DI*, as a function of the spectral displacement of the performance point, *Sd$_p$*. Median and 95% confidence level limit curves are shown. The spectral displacements obtained in Figure 27 are also depicted here.

Table 12. Median and 95% upper confidence level values of the expected spectral displacements, *Sd$_p$*, damage indices, *DI* and *d*, and damage probability matrices for two selected earthquake scenarios

	EARTHQUAKE SCENARIO FOR PGA = 0.11 g								
	Sd$_p$ (cm)	*DI*	*di*	P(*ds$_0$*)	P(*ds$_1$*)	P(*ds$_2$*)	P(*ds$_3$*)	P(*ds$_4$*)	P$_{TOT.}$
Median val.	10.6	0.21	0.84	0.39	0.42	0.16	0.03	***	1.00
95% conf.	13.4	0.42	1.68	0.11	0.32	0.36	0.18	0.03	1.00
	EARTHQUAKE SCENARIO FOR PGA = 0.24 g								
	Sd$_p$ (cm)	*DI*	*di*	P(*ds$_0$*)	P(*ds$_1$*)	P(*ds$_2$*)	P(*ds$_3$*)	P(*ds$_4$*)	P$_{TOT.}$
Median val.	18.7	0.73	2.92	0.01	0.06	0.23	0.42	0.28	1.00
95% conf.	23.2	0.86	3.44	***	0.01	0.08	0.35	0.56	1.00

(***) means very low probability.

This indicates a great uncertainty of this critical value, which is fundamental to estimate other sensitive and critical quantities, as for instance the numbers of expected casualties and homeless people. There is not a standard procedure to realize seismic risk assessment in a probabilistic way. The best procedure depends on the quantity and quality of the information availa-

ble. Uncertainties must be carefully analyzed and should be taken into account in an adequate way.

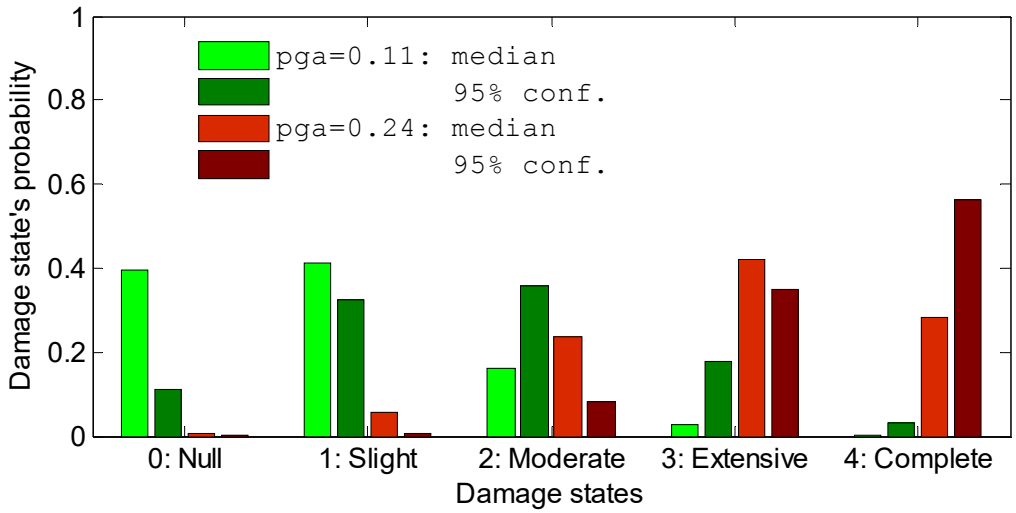

Figure 29. Damage probability matrices for PGA = 0.11 and 0.24 g. Median and 95% upper confidence levels are shown.

Low demanding scenarios may not be critical, as the influence of the uncertainties is lower, but for the analysis of intermediate and high demanding scenarios this influence may be crucial. When the quantity and quality of the data is adequate, for a given PGA, a suitable straightforward way to conduct such studies can follow these steps: **Step 1**: to use a probabilistic approach to obtain the performance spectral displacement, $Sd_{p,}$; to do that probabilistic capacity curves and probabilistic seismic actions can be used together; NLDA may be used but PA-8 procedure can be sufficient; as a result of this step the spectral displacement of the performance point, $Sd_{p,}$ for the selected PGA scenario is obtained as a random variable that includes the uncertainties of the seismic action and of the mechanical properties of the materials. **Step 2:** to take the spectral displacements of the performance point for the required confidence limits. **Step 3**: to use deterministic values, of the parameters of the building to get deterministic fragility curves; in this step different assumptions can be taken depending on the features of the actual buildings. For instance, mean, increased and decreased values of the mechanical properties of the materials or of other variables involved in the design and construction of the buildings can be used respectively for low-code, high-code and no-code buildings. **Step 4:** to use the median response spectrum of the seismic action to get the deterministic $DI(Sd_p)$ damage index function. **Step 5**: to determine the damage indices and the DPM for the required performance spectral displacements, Sd_p. Obviously other methods

based on Procedure B, as described above, can be used. In any case it is important to take special care in order not to take into account the uncertainties more than once and to make the adequate choice so as not to overestimate or underestimate the uncertainties involved in the seismic actions and in the mechanical and geometrical properties of the structure.

6.3 Conclusions

The main conclusions of this work are: 1) For low-to-moderate earthquakes, simplified deterministic static analysis methods can lead to quite good results when compared to more sophisticated NLDA, and 2) uncertainties in the input variables lead to significant uncertainties into the structural response and expected damage. These two main conclusions are described in more detail below. Concerning the comparison of nonlinear structural static and dynamic analyses, by using a deterministic model and characteristic values of the involved parameters, it can be concluded that, for the building analyzed herein, and for small-to-intermediate earthquakes, with a magnitude lower than 5.5, simplified static procedures lead to fairly good results, although they are somewhat conservative. The method, here known as PA-8, leads to more realistic results when compared to fully dynamic analysis. The equivalent linear displacement technique is very straightforward but may lead to quite conservative results, and therefore, in our view, the PA-8 technique is preferable. Furthermore, for intense seismic actions the use of fully dynamic analyses is justified. However, note that the two simplified methods are on the safety side. The probabilistic analyses confirm these conclusions. Concerning the influence that the uncertainties of the properties of the materials and those of the features of the seismic actions have on the uncertainties in the structural response, the main conclusions are outlined as follows. 1) All the results obtained with simplified and sophisticated structural analysis procedures show significant uncertainties in the computed output variables. It is important to observe that the coefficients of variation of the input variables used in this work are relatively small. 2) The correlation matrix between input and output variables provides valuable insights that can be useful not only in the design of new structures but also in the seismic risk assessment of existing ones. 3) The uncertainties in the response increase with the augment of the seismic actions due to the nonlinear behavior of the structural response; so, uncertainties in the capacity spectra increase with the spectral displacement, while uncertainties in the fragility curves increase with the damage state. 4) The major influence in the randomness of the structural response of the buildings comes from

the randomness of the seismic action; however the influence of the uncertainties on the mechanical properties of the materials is also significant. 5) The use of characteristic values in deterministic simplified approaches does not guarantee that the confidence level of the response be similar to that of the input variables. This fact is attributed to the nonlinear behavior of the structural system and it is evidenced by the significant differences between expected damage obtained from the spectral displacement calculated by means of nonlinear dynamic analysis. Specifically, the expected damage index obtained with the deterministic approach may become 20% lower than the expected damage index obtained with the probabilistic approach. Finally, it is important to remark that, regardless of the methodology, when assessing seismic vulnerability and expected damage, it is crucial to follow an approach that takes into account the nonlinear behavior of the structure, the randomness of the mechanical properties of materials and the uncertainties associated with seismic inputs.

Acknowledgements

The thoughtful comments of Professor Julian J. Bommer are kindly acknowledged. His comments and suggestions helped us to improve the manuscript and to address the probabilistic treatment of the seismic actions. This work has been partially funded by the Geologic Institute of Catalonia (IGC) and FEDER funds. The funding of the Spanish government and of the European Commission through research projects CGL2008-00869/BTE, CGL2011-23621, INTERREG: POCTEFA 2007-2013/ 73/08 and MOVE—FT7-ENV-2007-1-211590 is also acknowledged. Yeudy F. Vargas has a scholarship from an IGC-UPC joint agreement. The Spanish strong motion database has been provided by the Instituto Geográfico Nacional (IGN) Special thanks are given to Emilio Carreño and to Juan M. Alcalde, who provided us with the Spanish acceleration data, and to Ms. Maria del Mar Obrador who carefully reviewed the English.

References

Ambraseys, N., Smit, P., Sigbjornsson, R., Suhadolc, P. and Margaris, B. (2002), Internet-Site for European Strong-Motion Data, European Commission, Research-Directorate General, Environment and Climate Programme. http://www.isesd.hi.is/ESD_Local/frameset.htm (last accesed 2011-04-17).

Ambraseys, N., Smit, P., Douglas, J., Margaris, B., Sigbjornsson, R., Olafsson, S., Suhadolc, P. and Costa, G. (2004), Internet-Site for European Strong-Motion Data, *Bollettino di Geofisica Teorica ed Applicata*, **vol. 45, no. 3**, pp. 113-129.

ATC (1985). ATC-13. Earthquake damage evaluation data for California. Applied Technology Council, Redwood City, California. USA.

ATC (1991). ATC-25 Seismic Vulnerability and impact of disruption of lifelines in the conterminous United States. Applied Technology Council. Funded By Federal Emergency Management Agency. ATC. Redwood City. California. 1991. 440 pp.

ATC (1996) ATC-40. *Seismic evaluation and retrofit of concrete buildings*, Applied Technology Council, Redwood City, California.

Barbat A. H., Yépez Moya F. & J.A. Canas (1996) "Damage scenarios simulation for risk assessment in urban zones". *Earthquake Spectra*, 2(3), 371-394

Barbat A. H., Mena U. & F. Yépez (1998) "Evaluación probabilista del riesgo sísmico en zonas urbanas". *Revista internacional de métodos numéricos para cálculo y diseño en ingeniería*, 14(2), 247-268

Barbat A.H., Pujades L.G., Lantada N. & R. Moreno (2008) "Seismic damage evaluation in urban areas using the capacity spectrum method: application to Barcelona". *Soil Dynamics and Earthquake Engineering*, 28, 851–865.

Bommer, J.J. & H. Crowley (2006). The influence of ground motion variability in earthquake loss modelling. Bulletin of Earthquake Engineering 4(3), 231-248.

Borzi B., Phino R. & H Crowley (2008) "Simplified Pushover analysis for large-scale assessment of RC buildings". *Engineering Structures*. 30:804-820

Carr, A. J. (2000) "Ruaumoko-Inelastic Dynamic Analisys Program. Dept. of Civil Engineering". Univ. of Canterbury, Christchurch, New Zealand.

Chopra A.K. & R.K. Goel (1999) Capacity-Demand-Diagram Methods based on Inelastic Design Spectrum. *Earthquake spectra*, (15-4) 637-656.

Crowley, H., J.J. Bommer, R. Pinho & J.F. Bird (2005). The impact of epistemic uncertainty on an earthquake loss model. Earthquake *Engineering & Structural Dynamics* **34**(14), 1635-1685.

Dolsek M. (2010) "Effects of uncertainties on seismic response parameters of reinforced concrete frames". *Safety Reliability and Risk of Structures, Infrastructures and Engineering Systems*

EC08 (2004). EN-1998-1. Eurocode 8: *Design of structures for earthquake resistance -Part 1 General rules, seismic actions and rules for buildings*. English version. 232 pp.

Faccioli E (2006) Seismic hazard assessment for derivation of earthquake scenarios in Risk-UE. *Bull Earthq Eng* **4**:341–364

Faccioli E and V. Pessina (2003) *WP2–Basis of a handbook of earthquake ground motions scenarios,* Risk-UE project. WP-2 report. 99 pp.

Fajfar P. (1999) "Capacity spectrum method based on inelastic demand spectra". *Earthquake Engineering and Structural Dynamics*. 28:979-993

Faleiro J., Oller S. & A.H. Barbat (2008) "Plastic-damage seismic model for reinforced concrete frames". *Computers and Structures*. 86 (7-8), 581-597

Fragiadakis M. & D. Vamvatsikos (2010) "Estimation of Uncertain Parameters using Static Pushover Methods". in Proceedings of the tenth international conference on structural safety and reliability (icossar2009), osaka, japan, 13–17 september 2009 *Safety Reliability and Risk of Structures, Infrastructures and Engineering Systems* . Furuta H, Frangopol DM and M Shinozuka Eds. Taylor & Francis Group, London, UK. pp 659-660.

Freeman SA (1998) Development and use of capacity spectrum method. *Proceedings of the 6th US national conference on earthquake engineering*, Seattle, CD-ROM, EERI, Oakland.

Freeman SA (1978) Prediction of response of concrete buildings to severe earthquake motion. *Publication SP-55*, American Concrete Institute, Detroit, MI, 589-605.

Freeman SA, Nicoletti JP, Tyrell JV (1975) Evaluations of existing buildings for seismic risk—a case study of Puget Sound Naval Shipyard, Bremerton,Washington. *Proceedings of the 1st US national conference on earthquake engineering*, Oakland, California, pp 113–122

Gasparini D. & E.H. Vanmarcke (1976) "Simulated earthquake motions compatible with prescribed response spectra". *M.I.T. Department of Civil Engineering.* Research report R76-4, Order No. 527

Grünthal, G. (1998). "*European Macroseismic Scale 1998. EMS-98*". Conseil de L'Europe. Cahiers du centre Européen de Géodynamique et de Séismologie. Vol. 15.

FEMA (1997), *NEHRP guidelines for the seismic Rehabilitation of buildings,* FEMA 273; and NEHRP *Commentary on the Guidelines for Seismic Rehabilitation of Buildings*, FEMA 274, October, Federal Emergency Management Agency, Washington, D.C.

FEMA (1999) Earthquake Loss Estimation Methodology". HAZUS'99 (SR 2) *Technical Manual, Federal Emergency Management Agency (FEMA).* Washington D.C.

Hancock, J. & J.J. Bommer (2006) "A state of knowledge Review of the influence of strong motion duration on structural damage". *Earthquake Spectra.* Volume 22, No 3, 827-845.

Hancock, J., J.J. Bommer & P.J. Stafford (2008). Numbers of scaled and matched accelerograms required for inelastic dynamic analyses. *Earthquake Engineering & Structural Engineering* **37**(14), 1585-1607.

Hou, S. (1968) "Earthquake simulation models and their applications". *M.I.T. Department of Civil Engineering*. Research Report. R68-17

Kalos M. & P.A. Whitlock (1986) "Monte Carlo Methods". Volume I: Basics. ISBN 0-471-89839-2

Kim S.P. & Y.C. Kuruma (2008) "An alternative pushover analysis procedure to estimate seismic displacement demands". *Engineering structures*. 30:3793-3807

Lagomarsino S & S Giovinazzi S (2006) Macroseismic and mechanical models for the vulnerability and damage assessment of current buildings. *Bull Earthq Eng* 4:415–443

Lantada N, Pujades LG & A.H. Barbat (2009) "Vulnerability index and *capacity* spectrum based methods for urban seismic risk evaluation". A comparison. *Natural Hazards.* 51:501-524

Mahaney J.A. Paret T.F. Kehoe B.E. & S.A. Freeman (1993) "The capacity spectrum method for evaluating structural response during the Loma Prieta earthquake". *National earthquakes conference*, Memphis

Mwa*fy* A.M & A.S. Elnashai (2001) "Static pushover versus dynamic collapse analysis of RC buildings". *Engineering Structures*. 23:407–424

Mata P. A., Oller S. & A.H. Barbat (2007) "Static analysis of beam structures under nonlinear geometric and constitutive behaviour". *Computer Methods in Applied Mechanics and Engineering*. 196:4458-4478

McGuire RK (2004) *Seismic hazard and risk analysis.* Earthquake Engineering Research Institute. MNO-10. 221 pp.

Milutinovic ZV, Trendafiloski GS (2003) *WP04 Vulnerability of current buildings*. RISK-UE project of the EC: an advanced approach to earthquake risk scenarios with applications to different European towns

NCSE-02 (2002). Real Decreto 997/2002, de 27 de septiembre, por el que se aprueba la norma de construcción sismorresistente: parte general y edificación (NCSR-02). Ministerio de Fomento. Fecha de publicación: 11-10-2002. BOE: 244-2002. Pp. 35898-35966

Otani S (1974) Inelastic analysis of RC frames structures. *J. Struct. Div., ASCE* 100(7): 1433–1449.

Poursha M., Khoshnoudian F & A.S. Moghadam (2009) "A consecutive modal pushover procedure for estimating the seismic demands of tall buildings". *Engineering Structures*. 31:591-599

Pujades L.G., Barbat A.H., R. González-Drigo, Avila J. & S. Lagomarsino (2012) "Seismic performance of a block of buildings representative of the typical construction in the Eixample district in Barcelona (Spain) ". *Bulletin of Earthquake Engineering.* Vol. 10, pp 331–349.

RISK UE Project of the European Commission (2004) "An advanced approach to earthquake risk scenarios with applications to different European towns". Contract number: EVK4-CT-2000-00014

Satyarno I. (1999) "Pushover analysis for the seismic assessment of reinforced concrete buildings". Doctoral Thesis, Department of civil engineering, University of Canterbury.

SEAOC Vision 2000 Committee (1995). *Performance-Based Seismic Engineering*. Report prepared by Structural Engineers Association of California, Sacramento, California. Sacramento, CA. April 1995 final report.

Vamvatsikos D. & C.A. Cornell (2001) "The Incremental Dynamic Analysis". *Earthquake Engineering and Structural Dynamics*. 31(3): 491-514

Vargas Y.F., Pujades L.G., Barbat A.H. & J.E. Hurtado (2010) "Probabilistic Assessment of the Global Damage in Reinforced Concrete Structures". *Proceeding of the 14th European Conference on Earthquake Engineering, Ohrid August 2010*

Vielma J. C., Barbat A.H. & S. Oller (2009) "Seismic performance of waffled-slabs floor buildings". *Structures and Buildings (Proceedings of the Institution of Civil Engineering),* 162(SB3), 169-182

Vielma J. C., Barbat A.H. & S. Oller (2010) "Seismic safety of limited ductility buildings", *Bulletin of Earthquake Engineering*. 8(1), 135-155.

Villalba V (2006). *Introducción a los forjados*. http://www.salleurl.edu/tecnologia/pdf/teoria/tercer/09.pdf. (Last accessed 2012/11/18).

Vitruvius (1BC) *The ten books on architecture*. Translated by M.H. Morgan. Cambridge. Harvard University Press. 1914. 330 pp.